![aer logo]

Testing Variations of Exponential-Random Cloud Overlap with RRTMG in HWRF

Michael J. Iacono and John M. Henderson
Atmospheric and Environmental Research
131 Hartwell Avenue, Lexington, Massachusetts 02421-3126
(E-mail: miacono@aer.com)

Final Project Report

Developmental Testbed Center (DTC) Visitor Program 2018

February 2019

1. Overview

The main objective of this project for the Developmental Testbed Center Visitor Program was to implement and test revisions to HWRF (*Bernardet et al.*, 2015; *Biswas et al.*, 2018) related to the treatment of cloud radiative transfer in the RRTMG radiation code developed at AER (*Iacono et al.,* 2008). NOAA's Environmental Modeling Center (EMC) adopted RRTMG for operational use in HWRF_v3.7 during the 2015 hurricane season. ***Based in part on our recent work with DTC, EMC adopted the exponential cloud overlap method in RRTMG for operational use in HWRF during the 2018 hurricane season***. Further testing by the DTC and EMC in support of the operational use of the exponential-random cloud overlap method is currently pending. For this project, the specific cloud radiation change investigated related to the radiative coupling of clouds and the treatment of vertical cloud overlap, which can strongly impact radiative fluxes and heating rates. The default cloud overlap assumption in RRTMG, known as maximum-random (MR), has been compared to alternate methods known as exponential (EXP) and exponential-random (ER) to establish the impact of revising this cloud-radiative process on the prediction of tropical cyclones in HWRF. Forecasts of multiple tropical cyclones have shown a significant response in atmospheric heating rates due to cloud overlap changes that alters the atmospheric state to a sufficient degree that tropical cyclone track and intensity are affected in some cases.

Recommendations: The EXP and ER methods were each tested in two different forms that varied the specification of the required decorrelation length (DL). Although the modest scale of testing and validation that was accomplished during this visitor project was not extensive enough for us to draw final conclusions about which overlap configuration has the most potential to improve hurricane forecast skill with HWRF, which should be realized with more comprehensive testing, we can make the following recommendations:

1) For relative continuity with the widely used MR overlap, the ER method, if it performs better, should be considered a higher priority for general use than the EXP method,
2) The differences in TC forecasting impacts between EXP and ER will be smaller than the impact of either of these methods relative to MR overlap,
3) Larger scale testing should focus on using the ER method with the recommended constant DL (2500 m), followed by tests using ER with the latitude-varying DL,
4) Within the northern tropical latitudes (near 20° N), the latitude-varying DL for EXP and ER will be very close to the recommended constant DL, and thus these two variations will perform similarly at those latitudes; at much lower and higher latitudes, the latitude-varying DL for EXP and ER will be more likely to produce results that diverge from the constant DL method,
5) Both EXP and ER overlap show the potential for impacting the atmospheric state at synoptic and larger scales, and this result should be investigated more extensively.

Important Note: The cloud overlap method tested during our previous DTC effort and described in our final report for that project (dated March 2017) relates to the *exponential cloud overlap* method, although it was later found to be incorrectly labeled in that document as the exponential-random method. The distinction between these two methods and their relative impacts on tropical cyclones are described in further detail in this report.

2. Background

Cloud Overlap

The representation of the sub-grid scale properties of clouds in dynamical models remains a significant source of uncertainty in weather forecasts and climate projections. This uncertainty relates to the horizontal inhomogeneity of cloud microphysical properties and the vertical correlation or overlap of clouds and their impacts on cloud radiative processes. Understanding each of these effects is critical to simulations of the atmosphere (*Wu and Liang*, 2005). Biases associated with these processes have been shown to compensate to some degree (*Nam et al.,* 2012; *Shonk et al.,* 2010b), which reinforces the need both to study them independently and to improve them in combination.

Of importance to the project tasks is the application within RRTMG of the Monte-Carlo Independent Column Approximation (McICA; *Barker et al.*, 2007; *Pincus et al.*, 2003), which is a statistical technique for representing the sub-grid variability of clouds within the radiative transfer calculations. At present, McICA is used to represent the cloud fraction and vertical correlation of clouds. Cloud overlap assumptions in RRTMG include random (no correlation between disassociated, separated cloud layers), maximum (fully overlapping in the vertical within adjacent, multiple cloud layers), and a blend of these two called maximum-random (maximum overlap in adjacent cloud layers and random overlap among separated groups of cloud layers) first described by *Geleyn and Hollingsworth* (1979). During our previous DTC/VP project, RRTMG was modified to use the exponential-random (*Hogan and Illingworth*, 2000; *Shonk, et al.,* 2010a) cloud overlap method, which presumes that the vertical correlation within a group of adjacent cloud layers transitions inverse exponentially from maximum to random with increasing distance. The exponential-random (ER) method is in effect a compromise between the more extreme random and maximum-random (MR) assumptions. The ER approach defines the exponential transition, α, of cloud overlap from maximum to random within continuous cloud layers as a function of distance through the cloud, Δz, and a decorrelation length, Z_0:

$$\alpha = e^{-(\Delta z/Z_0)} . \qquad [1]$$

High decorrelation lengths ($\alpha \rightarrow 1$) infer a greater tendency toward maximum overlap, and low decorrelation lengths ($\alpha \rightarrow 0$) infer a greater tendency toward random overlap. Finely spaced vertical layering implies smaller values of Δz, higher α, and maximum overlap, while coarser vertical spacing corresponds to higher values of Δz, lower α, and more random vertical correlation. Through multiple adjacent cloudy layers, the vertical correlation trends toward random overlap as the exponential transition is applied at each layer. Our previous HWRF experiments used a constant decorrelation length of 2 km as a representative tropical value consistent with radar cloud measurements (*Pincus et al.,* 2005). In true ER overlap, the presence of clear layers between cloudy layers forces the exponential transition within non-adjacent blocks of cloudy layers to be randomly correlated with each other.

It came to our attention through documented radiation enhancements at ECMWF (*Hogan and Bozzo*, 2016) that the cloud overlap method used in our previous DTC research, which was based on the work of *Raisanen et al.* (2004), actually represents the exponential transition from maximum to random without regard to the presence of clear layers between blocks of cloudy layers. This variation, which hereafter will be termed exponential cloud overlap (EXP) is essentially the same assumption described by *Bergman and Rasch* (2002). The EXP method is equally valid for study within dynamical models, though it has a different effect on cloud radiative transfer than the intended ER method. As discussed by *Hogan and Bozzo* (2016), the EXP approach (which they refer to as EXP-EXP) generally underestimates total cloud cover relative to ER (when cloud layers are separated by clear layers), and in some configurations EXP can even underestimate total cloud cover relative to MR overlap. It is a simple matter to revise the previously tested EXP method to impose random correlation between separated cloudy layers by setting the vertical correlation between adjacent layers, α, to 0 when either layer, or both, is fully clear, and this revision will be tested in this project. Since the EXP method is identical to ER over adjacent cloudy layers that are not separated by clear sky, the impact of this change in deep tropical clouds in the vicinity of mature tropical cyclones may be negligible, though it may have more of an impact on the surrounding environment. It should be noted that the influence of EXP overlap in our 2016 VP work extended to the synoptic scale and is likely global, and we also expect this to be the case for the ER overlap revisions to be tested in the current work.

We will also examine two additional variations of ER overlap, one that uses different spatially constant values of decorrelation length (varying from 1.5 to 3.5 km) and another that allows the decorrelation length to vary spatially by latitude over a similar range. The latter variation applies lower decorrelation length values (~1.5 km) at higher latitude where cloud vertical correlation is more random and higher values (~3.5 km) at lower latitude where cloud vertical correlation tends toward maximum in deep convection. More sophisticated approaches that vary

the cloud overlap method directly as a function of one or more atmospheric state parameters or that vary the overlap by grid spacing and are scale aware are beyond the scope of this project, though they will be the subject of future HWRF investigations.
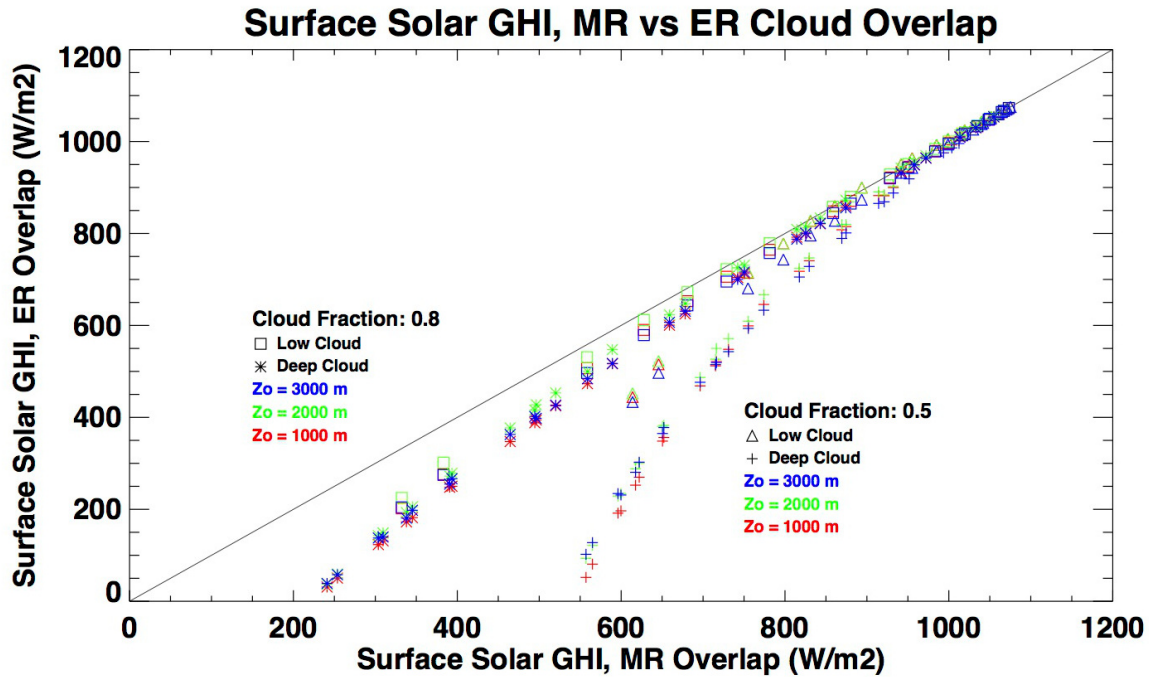
Figure 1. Surface solar global horizontal irradiance (GHI) calculated by RRTMG_SW using the ER cloud overlap method as a function of GHI calculated using MR overlap for two values of cloud fraction and a set of 49 cloud cases with varying cloud optical depth (low optical depth: high GHI; high optical depth: low GHI), two cloud vertical extents, low shallow cloud and deep cloud (symbols) and three ER overlap decorrelation lengths (colors).

The extent to which the ER method affects surface fluxes relative to MR overlap can be illustrated using idealized single-column calculations. Figure 1 illustrates the dependence of downward solar surface fluxes on cloud overlap by showing the global horizontal irradiance (GHI) calculated by RRTMG_SW using ER overlap as a function of the same calculations using MR overlap. The calculations covered a wide range of cloud optical depth using two cloud fractions (0.5 and 0.8 in each cloud layer), two cloud vertical extents (low shallow cloud and deep cloud), and three values of ER decorrelation length (1000 m in red, 2000 m in green, and 3000 m in blue). The overcast cloud result, for which the ER and MR approaches produce the same surface GHI is shown as the thin black diagonal line. This figure demonstrates that the GHI calculated with the two overlap methods diverges when cloud optical depths are high (corresponding to lower GHI), when cloud fractions are low (toward the right), when clouds have greater vertical extent ("*" and "+" symbols), and when smaller decorrelation lengths are used (red colors). Although the lower range of the y-axis in Figure 1 represents clouds of exceedingly high optical depth that may rarely occur in nature, GHI differences across the middle area of the plot (covering realistic cloud optical depths) are considerable.

4

Microphysics

Another essential component of effectively testing the radiative impacts of vertical cloud overlap assumptions is representing the distribution of partial cloudiness in the forecast model in a realistic way, since cloud overlap is only relevant in partial cloud conditions. Dr. Greg Thompson has advanced this aspect of HWRF with a cloud fraction parameterization (ICLOUD=3 namelist option), which provides a more realistic distribution of fractional cloudiness than the previously available options in WRF. Dr. Thompson has also upgraded the Thompson microphysics scheme to improve the coupling of cloud properties to the RRTMG radiation, by diagnosing the effective particle sizes of cloud water, ice and snow for the radiation code. Our experiments used the default HWRF microphysics scheme for the versions we applied. Our participation in the DTC Visitor Program continues to provide the opportunity to work with Dr. Thompson on evaluating and optimizing the representation of clouds and the interactions between the radiation and microphysics parameterizations in HWRF.

HWRF Configuration

During the course of this project, the DTC upgraded HWRF from the "H217" version (HWRF_v3.9a; *Biswas et al.*, 2017) to the "H218" version (HWRF_v4.0a; *Biswas et al.*, 2018). We completed TC forecasts using both versions in order to accomplish the proposed tasks while also seeking to inform the development of the 2019 operational HWRF model by DTC and EMC. Within both versions we continued to use the cloud fraction parameterization developed by Dr. Greg Thompson, which was designed to provide a more realistic distribution of fractional cloudiness in HWRF. The option is activated using the ICLOUD=3 WRF name-list setting. This option is especially relevant to the forecasts performed for this project, since the cloud overlap assumption used in the radiative transfer is strongly dependent on the sub-grid cloud fraction defined by the host model. All HWRF runs used the RRTMG longwave and shortwave radiation options. The three HWRF nested grids (where the outer grid is initialized with GFS model data) were used with the standard grid spacings of 18, 6, and 2 km (for H217) and 13.5, 4.5, and 1.5 km (for H218). Each of the tropical cyclones examined were forecast using multiple 126-hour forecast cycles that were initialized at 6-hour intervals. In each case, the initial forecast cycle was a "cold start" from GFS initial conditions and subsequent forecast cycles were a "warm start" in that the atmospheric state was derived from the previous forecast cycle (with the exception of the default vortex relocation at the start of each run). This arrangement ensured that the effects of the cloud overlap modifications were carried from one forecast cycle to the next through any atmospheric state changes. Finally, our runs with H217 used the 40-member HWRF ensemble to estimate the ensemble contribution to the background error covariance, while our runs with H218 used the GFS ensemble for this purpose to improve the efficiency of the runs while still providing a valid context for the assessment of the physics changes.
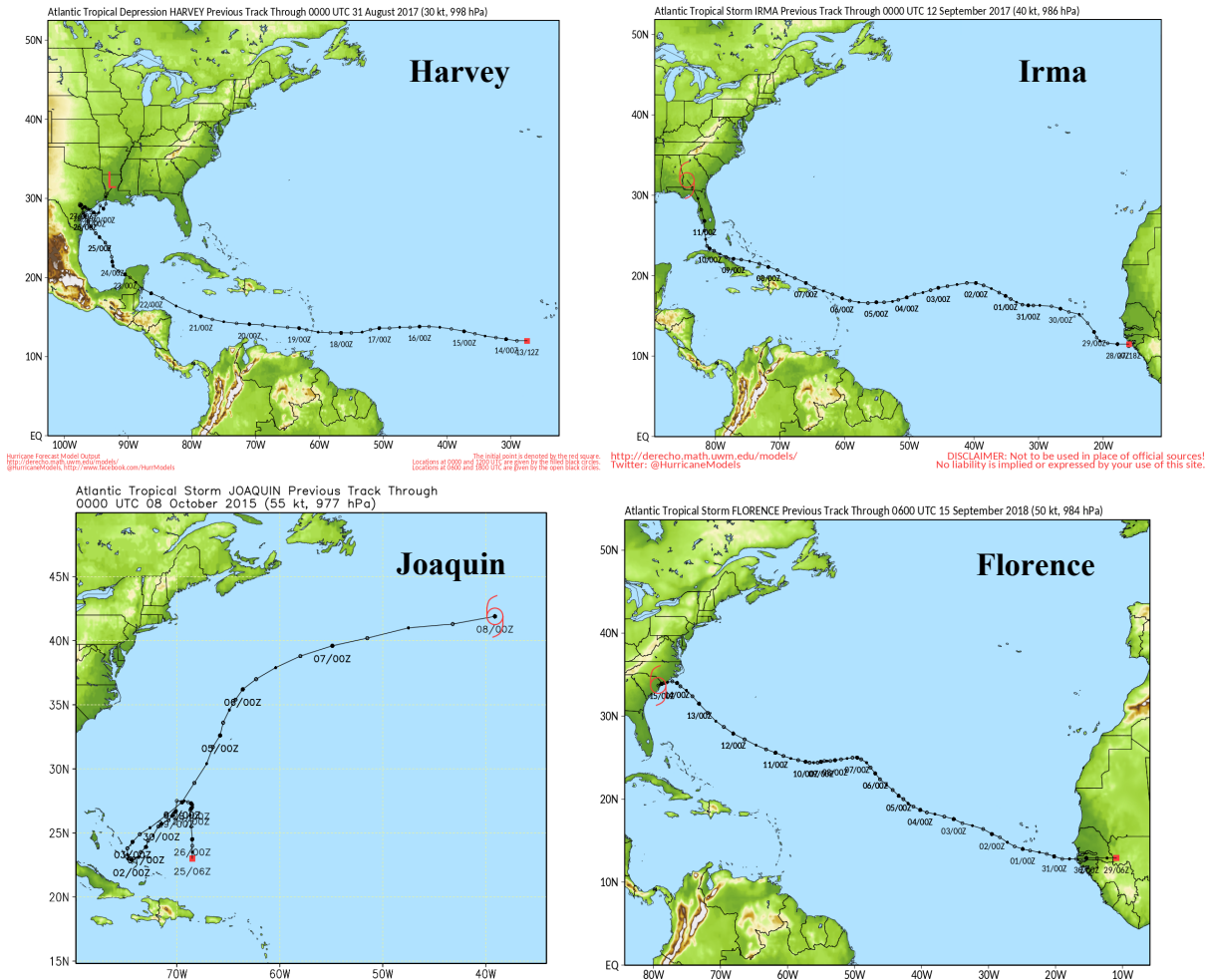
Figure 2. Best track paths of Hurricane Harvey through the western Atlantic basin from 13 August to 31 August 2017 (top left), Hurricane Irma across the Atlantic basin from 28 August to 12 September 2017 (top right), Hurricane Joaquin through the northwest Atlantic from 25 September to 8 October 2015 (bottom left), and Hurricane Florence across the Atlantic basin from 30 August to 15 September 2018 (bottom right).

Tropical Cyclone Cases

This project assessed the impacts of the cloud overlap change on the evolution of four tropical cyclone cases (Joaquin, Harvey, Irma, and Florence). Hurricane Joaquin was an Atlantic (ATL) basin TC that was active from 25 September to 8 October 2015 (*Berg*, 2016). This storm reached Category 4 intensity and followed a highly unusual track through the northwestern Atlantic, shown in Figure 2 (bottom left panel), which remained a forecasting challenge for many of the operational, hurricane forecast models through much of the storm's lifetime. This TC was examined for this project due the high sensitivity of its track and intensity to the EXP cloud overlap method that was documented in earlier work. Hurricane Harvey was a high-impact Atlantic basin TC that was active from 13 August to 1 September 2017 (*Blake and Zelinsky*, 2018). This hurricane experienced rapid intensification in the Gulf of Mexico and reached Category 4 intensity just prior

to landfall in Texas at 03 UTC on 26 August 2017. The track of Harvey is shown in the upper left panel of Figure 2. After landfall, it moved very slowly for several days over eastern Texas and brought record rainfall and extreme flooding to the area. Hurricane Irma (Figure 2, upper right panel) was another high-impact Atlantic basin TC that was active from 28 August to 12 September 2017 (*Cangialosi et al.*, 2018). This long-lived Cape Verde hurricane reached Category 5 intensity and made a total of seven landfalls, including four in the Caribbean at Category 5 before striking the Florida Keys at Category 4 and finally Marco Island in southwestern Florida as Category 3 on 10 September 2017. Irma was one of the strongest, most destructive and costliest hurricanes on record in the Atlantic. Hurricane Florence was another Cape Verde Atlantic basin TC that left the coast of Africa on 30 August 2018 and made landfall in North Carolina on 14 September 2018. This storm rapidly intensified from a tropical storm to a Category 4 hurricane in about 36 hours from 9-10 September 2018. Although it weakened to Category 1 by landfall, it was a high impact storm that caused catastrophic flooding over North and South Carolina.

3. Results and Discussion

Atmospheric Impacts: Radiative Heating Rates

Our initial objective in diagnosing the impact of replacing the MR cloud overlap assumption with the ER method on TC evolution is to demonstrate that the change sufficiently alters the longwave and shortwave radiative heating rates to affect the atmospheric environment. Along with surface fluxes, the radiative heating rates are the primary means by which the radiative transfer influences the atmosphere. So, the cloud overlap modification is unlikely to affect TC evolution unless it first alters the vertical heating rate profiles. In addition, the radiative heating rate profile contains information related to all of the atmospheric parameters that were input into the radiation code, such as temperature, gas concentrations, cloud properties, etc. and the details of the heating rates provide substantial information about the radiative influence of these parameters on the atmospheric state and TC structure.
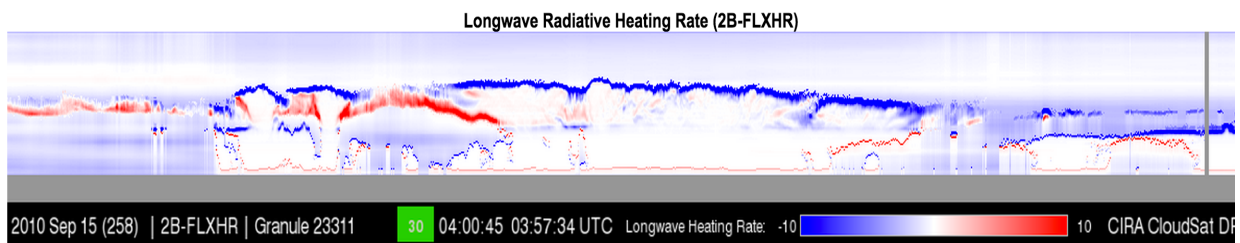
Figure 3. Longwave heating rate vertical cross section as derived from NASA CloudSat measurements for an intercept along the satellite path through Hurricane Julia at 04 UTC on 15 September 2010. Red denotes longwave heating and blue denotes longwave cooling.

Few opportunities are available to validate modeled radiative heating rate (HR) profiles with observations, though a derived heating rate product is available that is based on measurements from the NASA CloudSat instrument. These products consist of vertical slices along the satellite

path such as the longwave heating rate cross-section through Hurricane Julia taken at 04 UTC on 15 September 2010 shown in Figure 3. A database of all such intercepts through tropical cyclones has been made available (*Tourville et al.*, 2015). Application of these data to validating HWRF modeled heating rates near TCs will be addressed in future research.

In the style of the CloudSat vertical cross-section heating rate product, changes in modeled radiative heating rates due to exchanging the cloud overlap method were examined by looking at vertical slices through tropical cyclone Irma during both its developing and mature phases. Figure 4 shows a height-by-longitude slice of longwave heating rate directly through the center of developing Tropical Storm Irma as predicted by H217 using MR overlap (top panel) averaged over a 12-hour period from 12 UTC 30 August 2017 to 00 UTC on 31 August 2017. Also shown in Figure 4 are longwave heating rate differences for EXP-MR (center panel) and ER-MR (bottom panel) to highlight the impact of each overlap change at this development stage of Irma. Heating rate data are plotted from the moving inner grid, which remained centered on the TC, and over the time period shown the best track position of the center of Tropical Storm Irma moved directly westward from 16.3°N, 29.7°W to 16.3°N, 31.7°W and strengthened from having sustained winds near 50 mph to 60 mph. At this stage in its development, Irma has not yet developed any sign of a central eye though its cloud structure has greatly altered the background longwave heating rate pattern seen outside the region of the storm (westward of 32°W and eastward of 28.5°W), which generally shows longwave cooling within clear sky through much of the middle to lower troposphere over a layer of low-level cumulus just above the surface. Slight heating near the tropopause suggests a layer of high clouds across this scene. Within the storm, longwave heating, indicating clouds, extends up to the upper troposphere with the freezing level apparent just above 600 hPa. Both the EXP and ER cloud overlap methods alter this pattern of longwave heating primarily in the upper levels of the TC where partial cloudiness is more likely. Differences between EXP and ER are also apparent, especially in the upper central areas of Irma.

Comparable longwave heating rates and differences for Irma as predicted by H217 using the three cloud overlap methods are shown in Figure 5 averaged over the fourth day (a 24-hour period) of a forecast cycle that was initialized at 12 UTC on 3 September 2017. At the start of this day, Irma was close to its peak intensity with sustained winds of 185 mph and a central pressure of 915 hPa then weakened slightly over this 24-hour period (from 12 UTC on 6 September 2017 to 12 UTC on 7 September 2017) as it moved north of the northern Caribbean islands from 18.1°N, 63.3°W to 20.2°N, 69.0°W. The impressive eyewall of Irma during this time is clearly apparent in the longwave heating rate derived using MR overlap (top panel in Figure 5) as an area of largely clear air (longwave cooling) within the eye and dense cloud (longwave heating) in the eyewall and the surrounding areas of the TC. The "stadium effect" in which the diameter of the eye increases

8
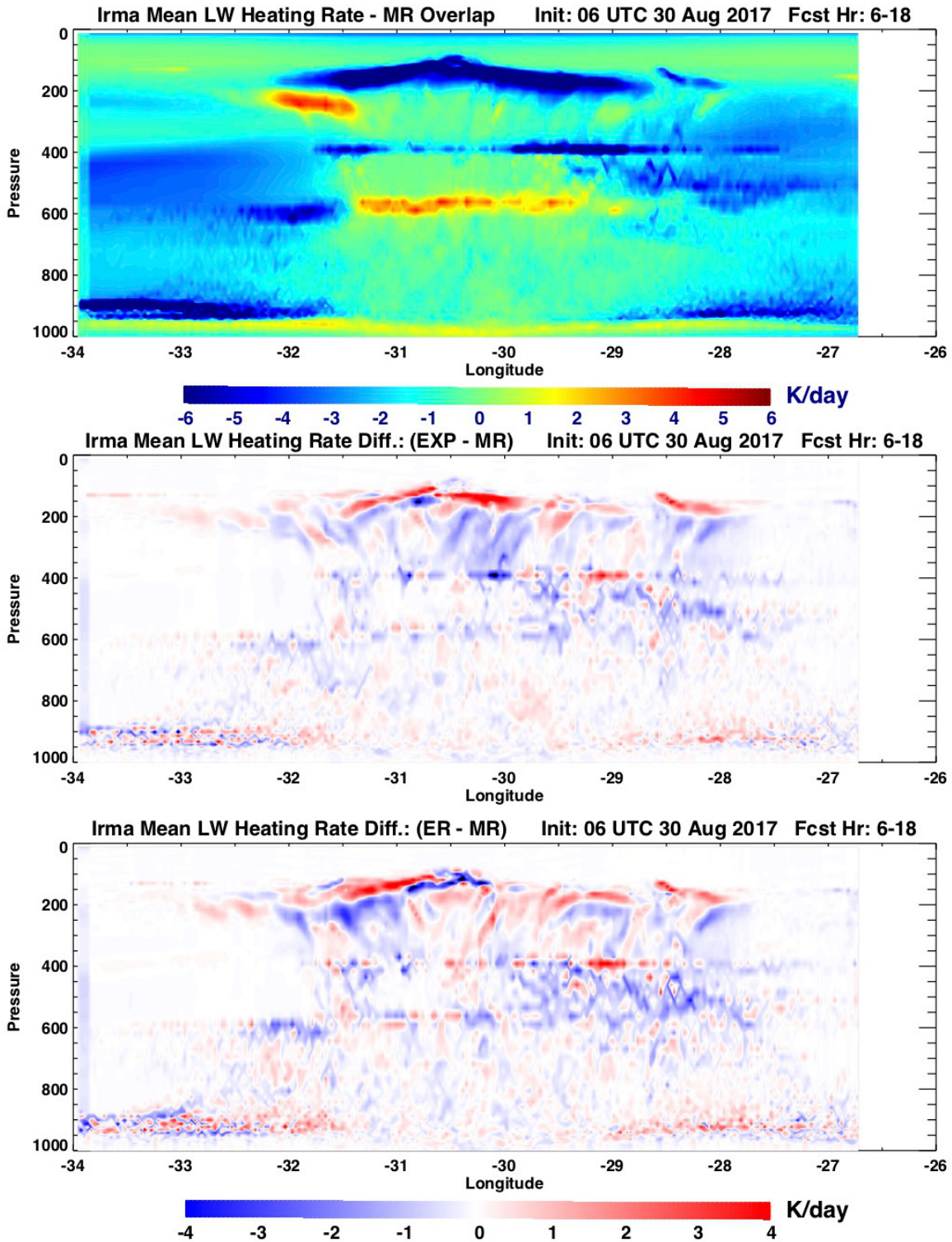
Figure 4. Height-by-longitude cross-sections of longwave heating rate as predicted by H217 using MR cloud overlap (top) and longwave heating rate differences for EXP-MR (center) and ER-MR cloud overlap (bottom) over the inner HWRF grid averaged over the 12-hour period from 12 UTC on 30 August 2017 to 00 UTC on 31 August 2017 directly through the center of Tropical Storm Irma. Units are Kd^{-1}.

9
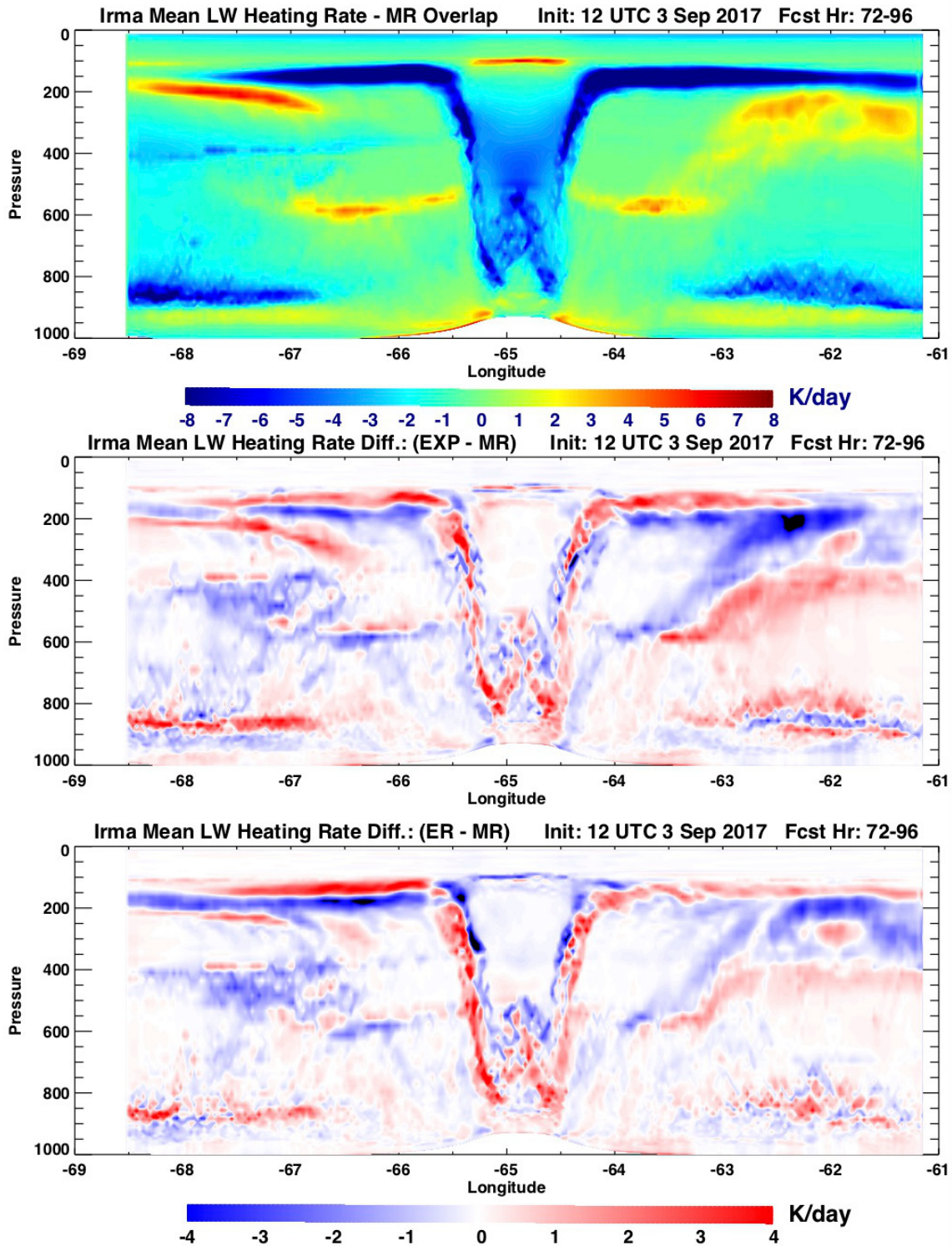
Figure 5. Height-by-longitude cross-sections of longwave heating rate as predicted by H217 using MR cloud overlap (top) and longwave heating rate differences for EXP-MR (center) and ER-MR cloud overlap (bottom) over the inner HWRF grid averaged over the 24-hour period from 12 UTC on 6 September 2017 to 12 UTC on 7 September 2017 directly through the center of Category 5 Hurricane Irma. Units are Kd^{-1}.

with height is also clearly visible. The effect on the longwave heating rate of replacing MR overlap is shown as differences for EXP-MR (center panel) and for ER-MR (bottom panel). Substantial shifts in the radiative heating rate patterns are noted in both cases implying changes in storm structure related cloud cover, temperature, moisture and other parameters that have altered the height of the clouds within the outflow at the top of the storm, the width of the eye (alternating red and blue in the eyewall in the difference plots), and the distribution of heating within the eastern part of the storm.

It is informative to compare the preceding HR plots with the cloud fractions generated by each forecast at the same place and time. Height-by-longitude plots of layer cloud fraction are shown in Figure 6 for the same vertical slice through Hurricane Irma shown in Figure 5 near its peak intensity for predictions using the MR overlap and for EXP-MR and ER-MR cloud fraction differences. Shown as fractions from 0 to 1, the layer cloud fractions in the top panel of Figure 6 illustrate the extent of fractional cloudiness that is present throughout the TC in the lower troposphere (with the notable exceptions of the eye wall and scattered overcast patches) where the cloud overlap change can potentially act to influence the atmosphere. Partial cloud cover in the lower atmosphere within Irma rapidly switches to overcast cloud above roughly 600 hPa, and this transition is apparent in the longwave heating rates shown in Figures 4 and 5. It should be noted that even where overcast clouds are present, the radiative heating rates may be influenced by changes in other atmospheric state parameters that have evolved during the forecast. Substantial differences in cloud fractions caused by the EXP and ER overlap methods relative to MR are shown in the lower panels of Figure 6. Cloud fraction changes of up to 50 percent are seen within the eyewall area (possibly reflecting differences in the diameter of the eye, and throughout much of the areas of the hurricane that are not overcast. An exception is the persistence of clear sky within the upper part of the eye and in the far outer regions of the TC that remain for all three cloud overlap methods. Differing cloud fractions are apparent at the top of the eye for EXP and ER with much smaller variations of cloud fraction within the outflow region.

Shortwave heating rate cross sections through the center of Hurricane Irma as predicted by H217 for the three cloud overlap methods are shown in Figure 7 for the same forecast cycle and averaged over the same forecast day as the longwave heating rates shown in Figure 5. Near neutral areas of shortwave heating in the top panel of Figure 5 indicate areas of cloudiness, while regions of positive heating reflect either strong shortwave clear-sky absorption (such as in the stratosphere) or strong scattering from clouds. The EXP and ER overlap methods show large differences in shortwave heating within the eye and eyewall of Irma, in the vicinity of the low-level convection in the outer parts of the storm and within a level of strong scattering near 400 hPa.

11
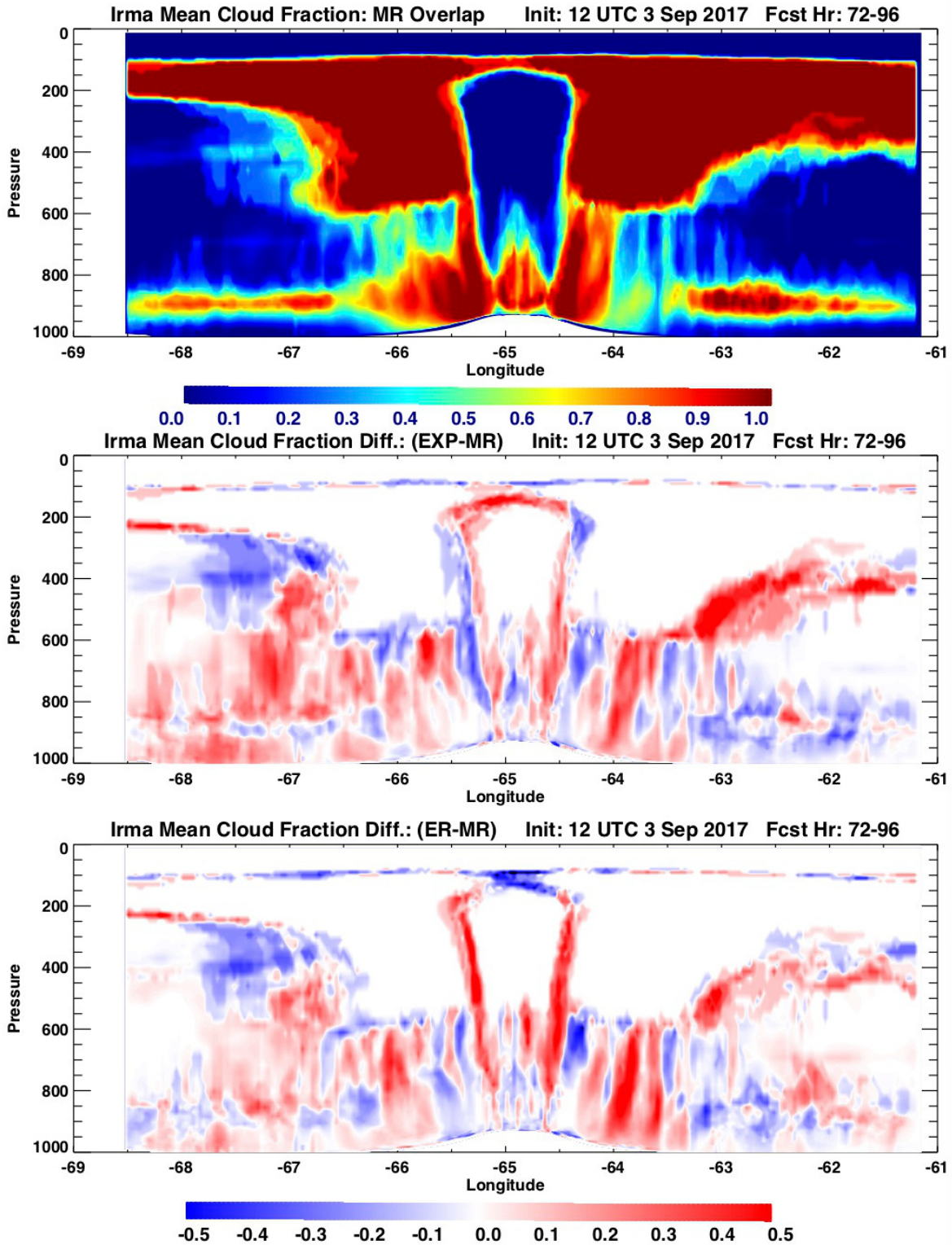
Figure 6. Height-by-longitude cross-sections of cloud fraction as predicted by H217 using MR cloud overlap (top) and cloud fraction differences for EXP-MR (center) and ER-MR (bottom) over the inner HWRF grid averaged over the 24-hour period from 12 UTC on 6 September 2017 to 12 UTC on 7 September 2017 directly through the center of Category 5 Hurricane Irma. Units are in fraction.
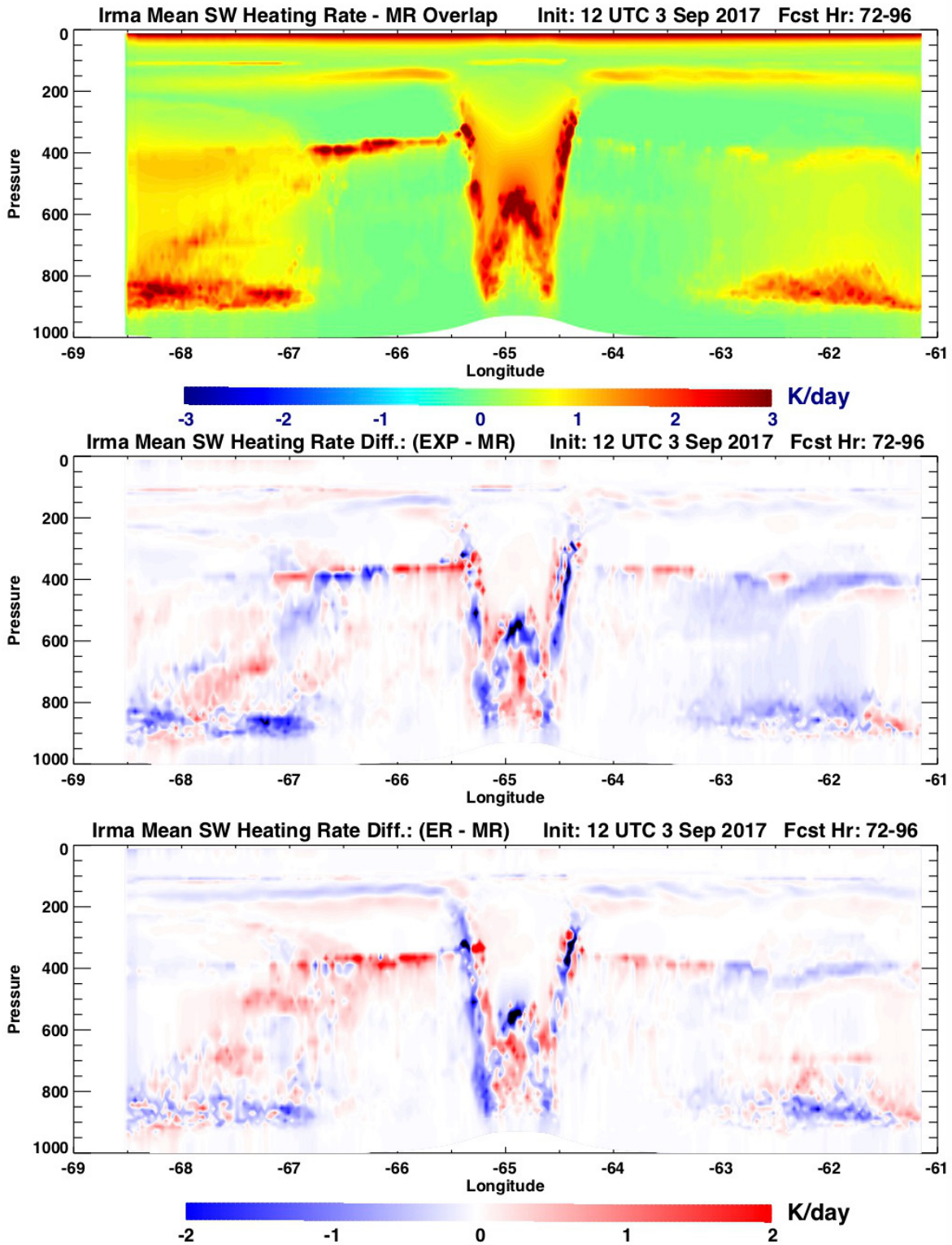
Figure 7. Height-by-longitude cross-sections of shortwave heating rate as predicted by H217 using MR cloud overlap (top) and shortwave heating rate differences for EXP-MR (center) and ER-MR cloud overlap (bottom) over the inner HWRF grid averaged over the 24-hour period from 12 UTC on 6 September 2017 to 12 UTC on 7 September 2017 directly through the center of Category 5 Hurricane Irma. Units are Kd^{-1}.
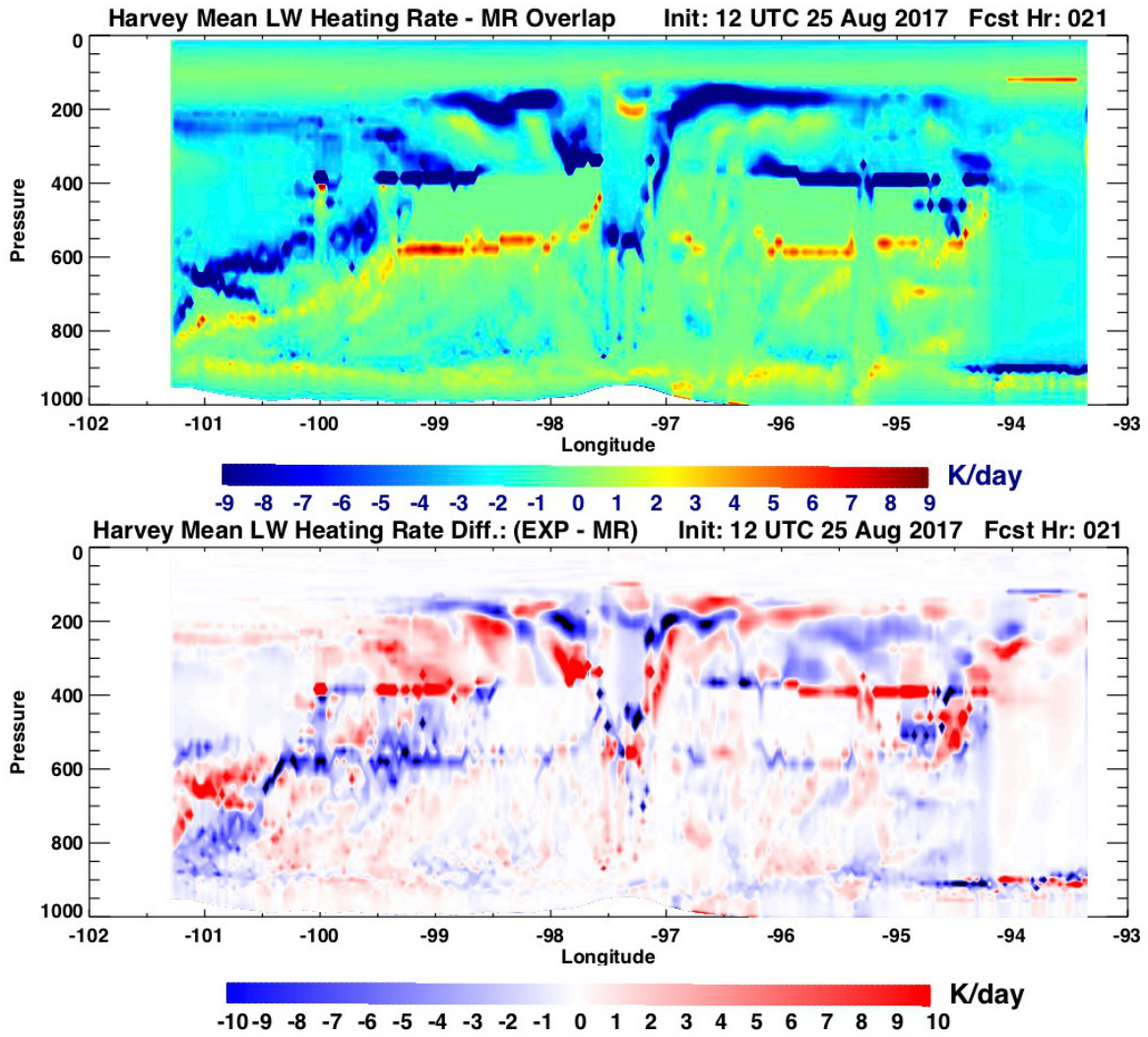
Figure 8. Height-by-longitude cross-sections of longwave heating rate as predicted by H217 using MR cloud overlap (top) and longwave heating rate difference for EXP-MR (bottom) over the inner HWRF grid at 09 UTC on 26 August 2017 directly through the center of Hurricane Harvey shortly after landfall. Units are Kd^{-1}.

A final longwave heating rate cross-section example is presented in Figure 8, which shows a snapshot in time of longwave heating through the center of Hurricane Harvey as predicted by H217 using MR cloud overlap (top panel) and for the EXP-MR difference (bottom panel) at 09 UTC on 26 August 2017 shortly after the storm made landfall on the coast of Texas. A H217 forecast using ER cloud overlap was not generated for this hurricane. Much larger heating rate differences are seen compared to Figures 4 and 5 since this plot is not averaged over time. Very apparent in Figure 8 are the erosion of the lower part of the eye of Harvey and the disruption of the outflow and the intrusion of clearer and drier air in the western section of the storm as the TC moved westward over land.
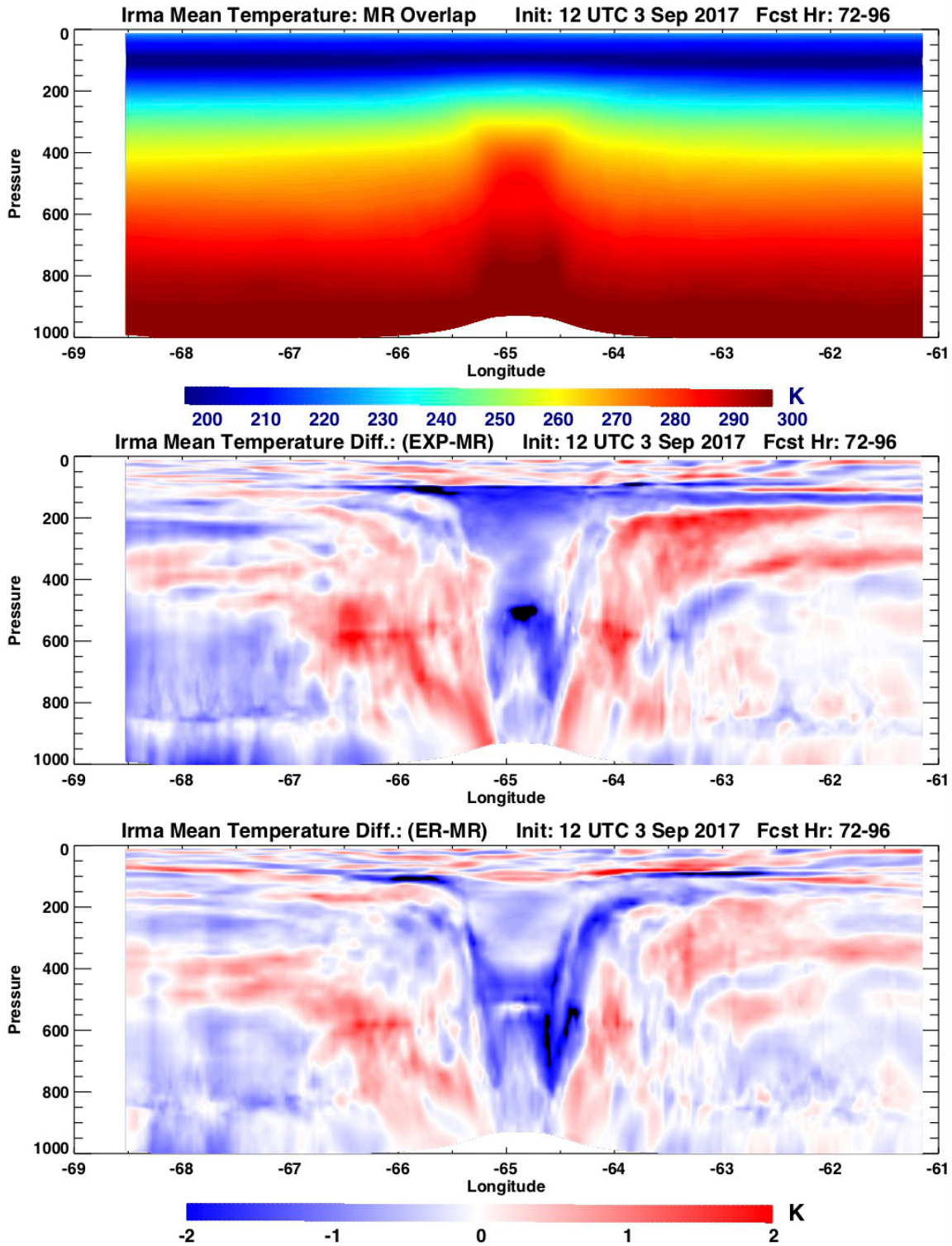
Figure 9. Height-by-longitude temperature cross-sections as predicted by H217 using MR cloud overlap (top) and temperature differences for EXP-MR (center) and ER-MR (bottom) over the inner HWRF grid averaged over the 24-hour period from 12 UTC on 6 September 2017 to 12 UTC on 7 September 2017 directly through the center of Category 5 Hurricane Irma. Units are in K.

15
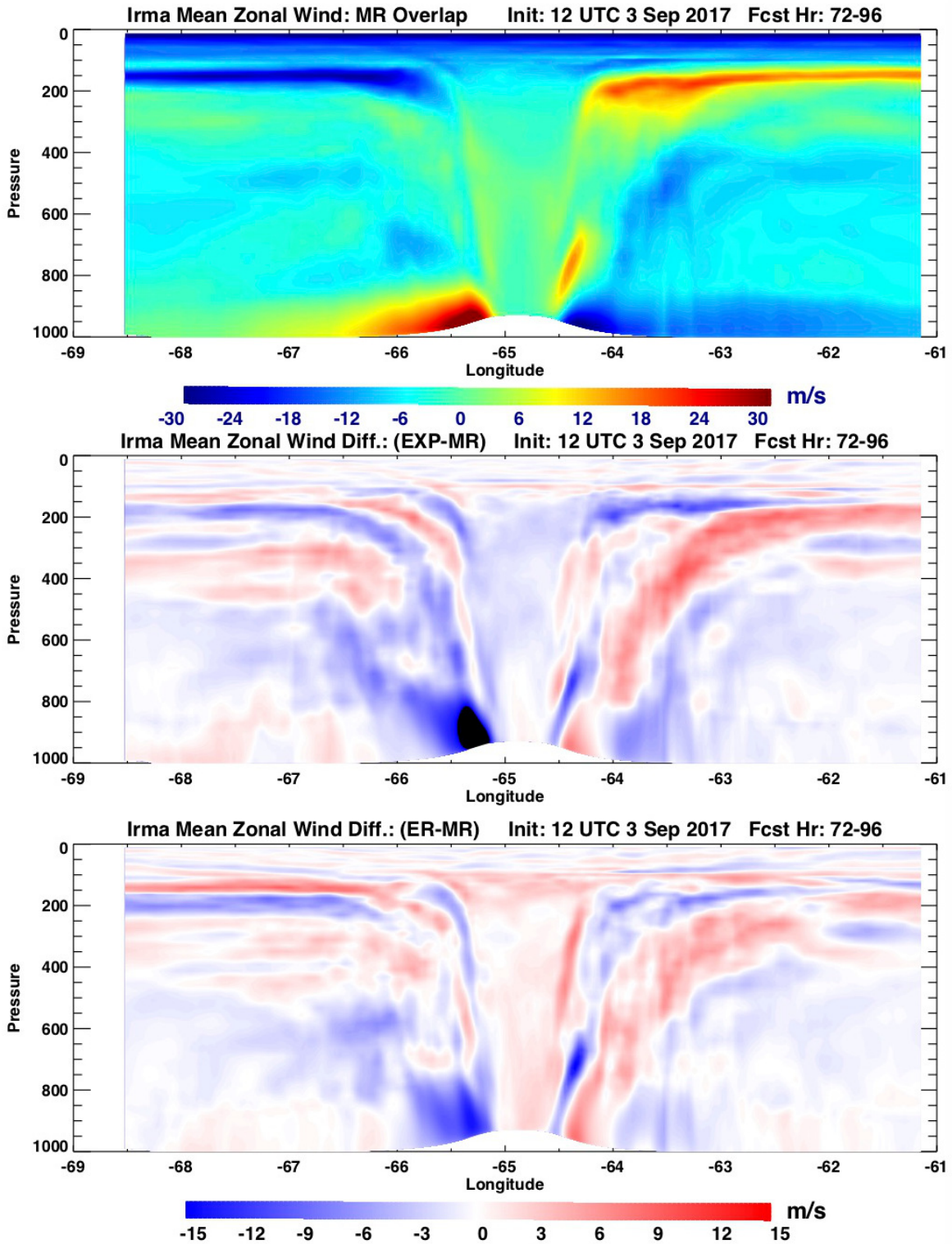
Figure 10. Height-by-longitude zonal wind cross-sections as predicted by H217 using MR cloud overlap (top) and zonal wind differences for EXP-MR (center) and ER-MR cloud overlap (bottom) over the inner HWRF grid averaged over the 24-hour period from 12 UTC on 6 September 2017 to 12 UTC on 7 September 2017 directly through the center of Category 5 Hurricane Irma. Units are ms^{-1}.

16

Atmospheric Impacts: Temperature and Wind Speed Cross-Sections

Vertical cross sections of temperature and temperature difference within Hurricane Irma averaged over the same forecast day as Figures 5-7 are shown in Figure 9. Both the EXP and ER overlap methods have introduced considerable changes in the temperature structure throughout the storm. A colder central eye is apparent for both the EXP and ER solutions for this forecast cycle relative to MR, though different parts of the eye are impacted in each case. Warmer areas within the eyewall and the surrounding interior of Irma are also seen, though the affected areas are warmed to a greater degree in the forecast using EXP. Temperature changes are also apparent within the upper part of the eye and in the outflow that are somewhat larger in the EXP solution. These temperature differences relate to adjustments in the structure of the storm such as the width of the eye, the position of the outflow level and the overall intensity, which these plots suggest is somewhat lower in the EXP and ER solutions relative to MR at this forecast time.

Vertical slices of the zonal and meridional wind speeds within Hurricane Irma for the same forecast day as above are shown, respectively, in Figures 10 and 11. The pattern of zonal winds for MR in the top panel of Figure 10 shows a positive (eastward) component to the west of the eye and a negative (westward) component to the east of the eye near the surface with the opposite pattern in the upper levels of the TC, which suggest the expected features of strong inflow near the surface and outflow near the top of the storm. Both EXP and ER reduce the strength of the zonal wind to the west of the eye near the surface, though to the east of the eye the zonal wind speed appears to be shifted more than weakened. The outflow in the zonal wind has been shifted downward slightly by the EXP and ER methods. The meridional wind speed using MR (top panel of Figure 11) shows the expected pattern of strong northly winds to the east of the eye and strong southerly winds to the west of the storm center. Using EXP overlap, the meridional wind speeds have been decreased around the storm center from the surface to the outflow region. Using ER overlap, the meridional winds appear to have shifted inward toward the center slightly, suggesting a slight decrease in the diameter of the ring of strongest wind speeds

For comparison to the meridional wind speeds in Figure 11 (while Irma was a hurricane) and the longwave heating rates in Figure 4 (when Irma was a tropical storm), the vertical cross sections of meridional wind speed and wind speed differences through Tropical Storm Irma are shown in Figure 12 for the same 12-hour average from the same forecast cycle as in Figure 4. At this early stage in its development, Irma showed widespread cyclonic flow across the plotted area through much of the troposphere as seen in the top panel of Figure 12. At the center of the storm, a sharp gradient of cyclonic wind shear is present across a very small distance of about 10 km. After only 6-18 forecast hours, the predictions using the EXP and ER methods already show significant differences in development from the MR solution (note the difference in the wind speed
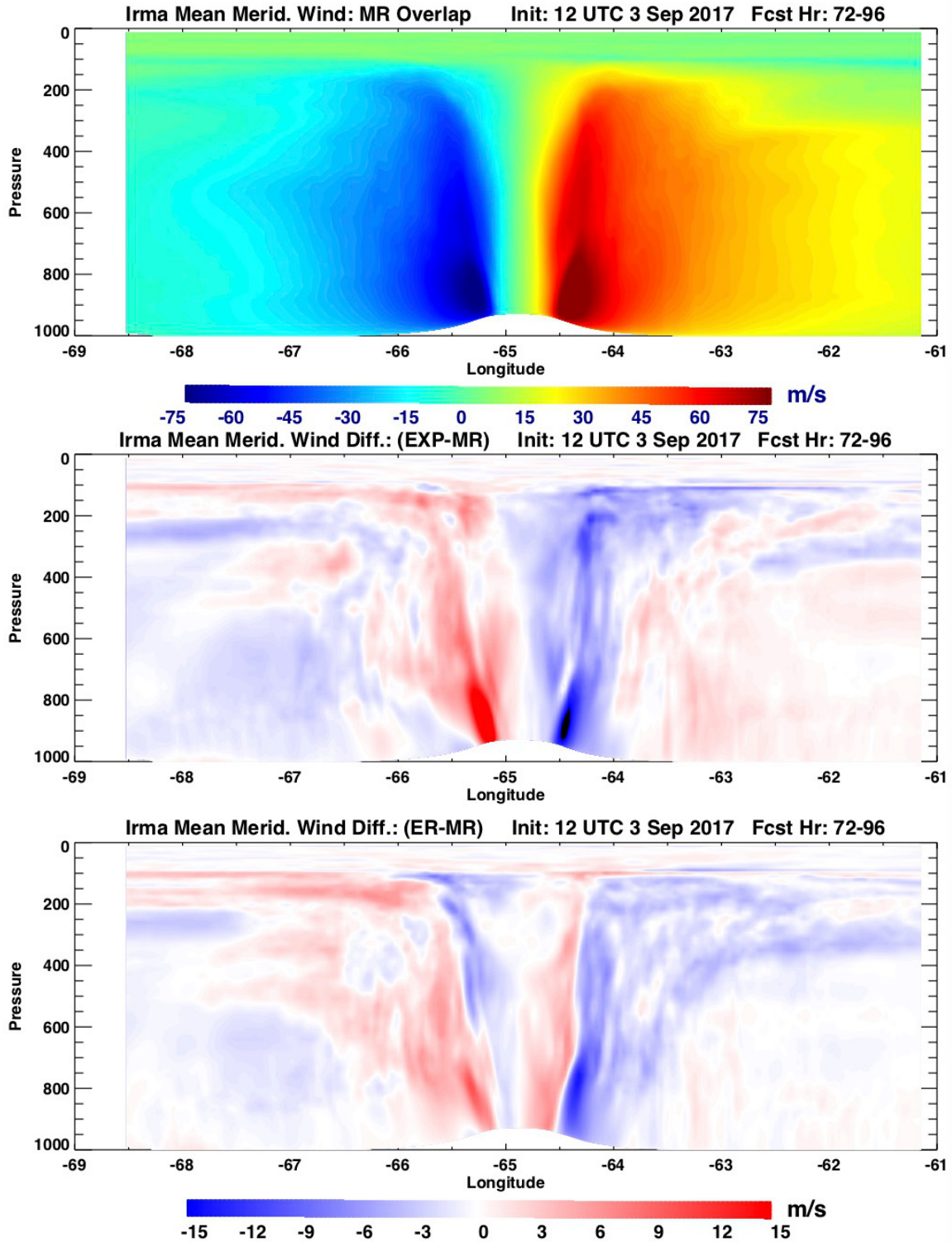
Figure 11. Height-by-longitude meridional wind cross-sections as predicted by H217 using MR cloud overlap (top) and meridional wind differences for EXP-MR (center) and ER-MR (bottom) over the inner HWRF grid averaged over the 24-hour period from 12 UTC on 6 September 2017 to 12 UTC on 7 September 2017 directly through the center of Category 5 Hurricane Irma. Units are ms^{-1}.

18
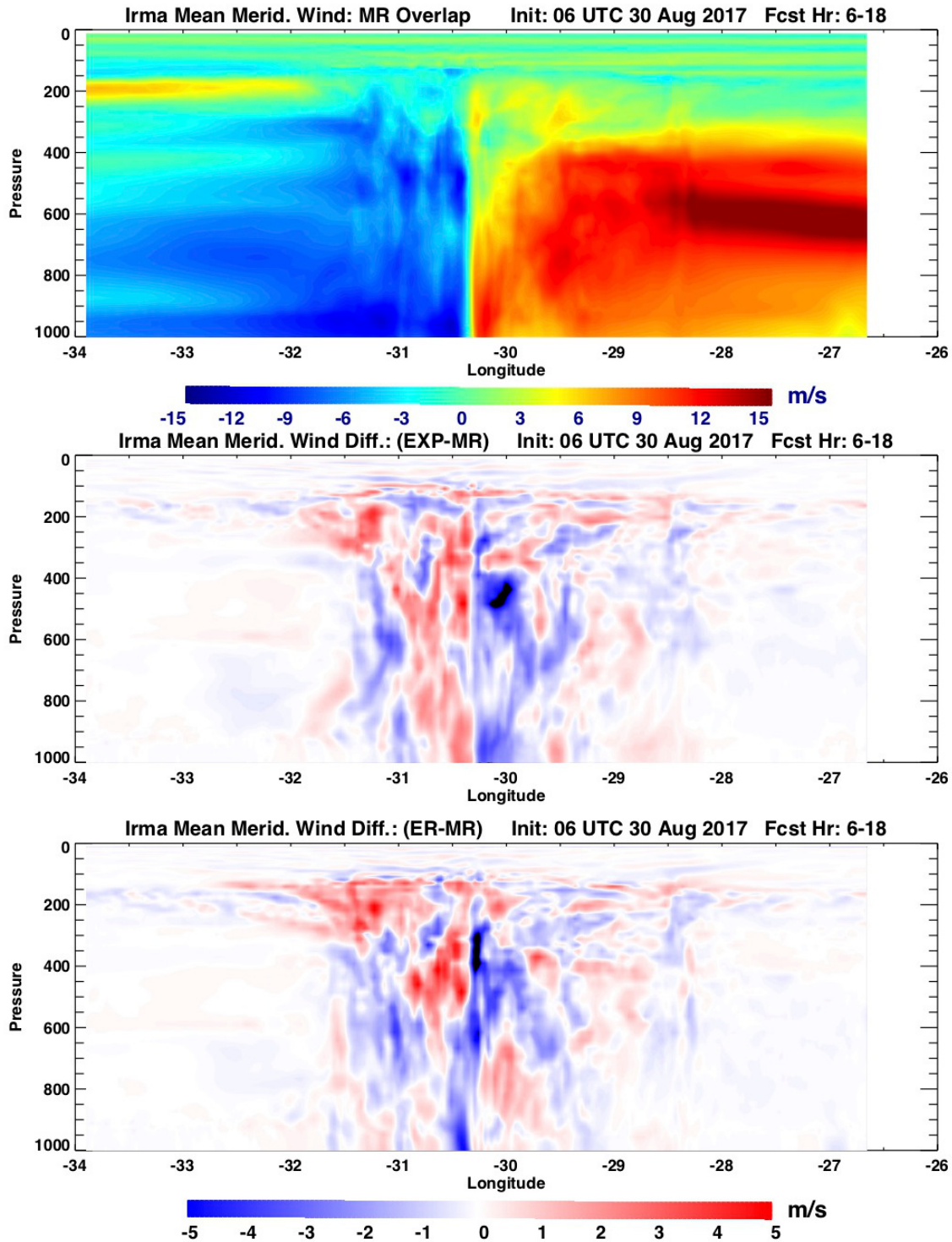
Figure 12. Height-by-longitude meridional wind cross-sections as predicted by H217 using MR cloud overlap (top) and meridional wind differences for EXP-MR (center) and ER-MR (bottom) over the inner HWRF grid averaged over the 12-hour period from 12 UTC on 30 August 2017 to 00 UTC on 31 August 2017 directly through the center of Tropical Storm Irma. Units are ms^{-1}.

scales between Figures 11 and 12). For EXP, the cyclonic flow has been weakened near the storm center up to about 400 hPa, while for ER, the circulation is weaker in the middle troposphere, but slightly intensified in the lower troposphere.

Atmospheric Impacts: Temperature and Wind Speed HWRF/GFS Comparison

A basic form of verification of the H218 forecasts with the new cloud overlap methods can be performed by comparing the hurricane model predictions to the GFS analysis used to initialize H218 at that time for a subsequent forecast cycle. Since the models produce output at different horizontal resolutions and different vertical layering, the differences were accomplished by interpolating the H218 output from sigma levels to match the GFS standard pressure levels, and both H218 and GFS were spatially interpolated to the same regular grid with a resolution of 0.1 degrees. Figure 13 shows 850 hPa temperature differences for the synoptic environment around Hurricane Joaquin between four H218 forecasts using the same four cloud overlap configurations presented in prior figures at forecast hour 96 from a cycle initialized at 00 UTC on 30 September 2015 and the GFS analysis used to initialize a later forecast cycle that began on 00 UTC 4 October 2015. The gray area in the lower left corner of each panel in Figure 13 represents missing GFS analysis data. Although all four overlap methods show significant H218 temperature differences at this level relative to GFS, differences among the four overlap methods are relatively small. One exception is the location of the hurricane itself, which was initialized by GFS close to its best track position at 00 UTC 4 October 2015 near 27.4°N and 69.5°W (visible as the small dark blue dot near the center of each panel) and was predicted by H218 to be significantly further north at this time (red areas near 32°N and 69°W in each panel). Since the plotted temperature differences are H218 – GFS, the location of the hurricane as predicted by H218 appears red (H218 warmer than GFS) while the location of the hurricane in the GFS analysis appears blue (GFS warmer than H218). It is also notable that H218 with the EXP and ER overlap methods predicts substantially different temperatures within the feature to the north through northeast of the hurricane (along 45°N), though the variations among the four overlap configurations presented is small. It should be noted that GFS also runs with the RRTMG radiation code, though it would have used the MR cloud overlap in its forecasts. A similar comparison of the 200 hPa meridional wind for the same models and forecast times as Figure 13 is shown in Figure 14. As with the temperature, the meridional winds predicted by H218 with EXP or ER differ over broad areas relative to the GFS analysis. The error in the storm location in the H218 forecast at this time is indicated by the couplets of positive/negative wind speed difference near the respective storm centers.

Temperature differences at 850 hPa are shown in Figure 15 for the synoptic environment around Hurricane Irma between H218 forecasts using the four cloud overlap configurations at forecast hour 96 from a cycle initialized at 12 UTC on 3 September 2017 and the GFS analysis
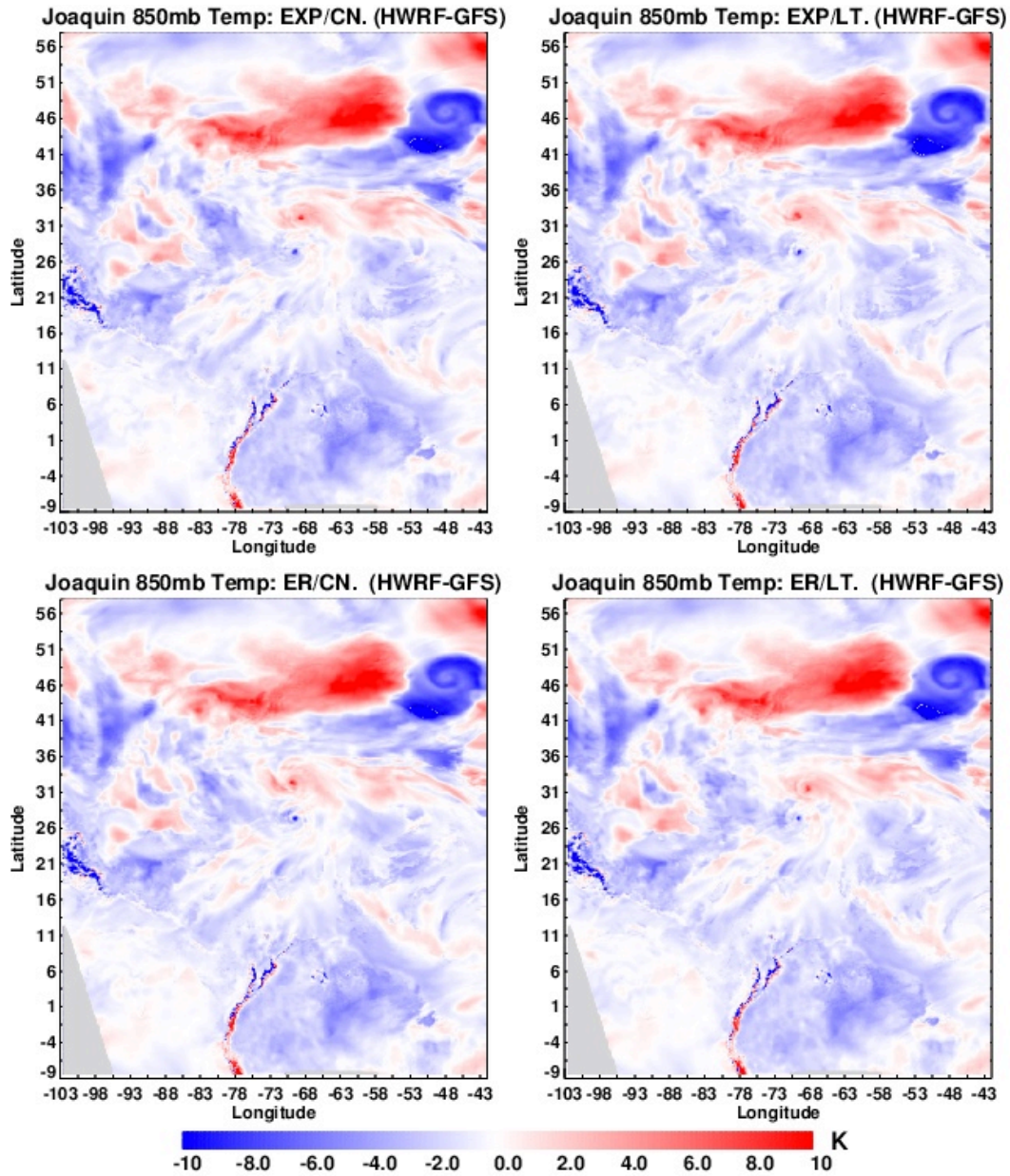
Figure 13. Temperature differences at 850 hPa of the synoptic environment around Hurricane Joaquin at 00 UTC on 4 October 2015 between H218 96-hour predictions at that forecast time and the GFS analysis at that time with H218 using EXP overlap with constant decorrelation length (top left), using EXP overlap with a latitude-varying decorrelation length (top right), using ER overlap with constant decorrelation length (bottom left), and using ER overlap with a latitude-varying decorrelation length (bottom right). Units are K. Gray areas denote missing data.

used to initialize a later forecast cycle that began on 12 UTC 7 September 2017. The gray area along the bottom and right edges of each panel in Figure 15 represents missing GFS analysis data. As with the previous example, H218 temperatures relative to GFS at this level among the four cloud overlap methods are very small and are most noticeable near the TC center, which is slightly further east of the analyzed position near 20.2°N and 69.0°W at this time. Warmer temperatures

21

are apparent in the H218 predictions within the northern part of the circulation of Irma. A comparison of the meridional wind speed differences at this time for Irma are shown in Figure 16. The eastward bias in the H218 location of the center of Irma is very apparent by the couplet of negative/positive wind speed values indicating stronger northward winds further east and stronger southward winds further west in H218 relative to the analyzed center. In addition, another feature
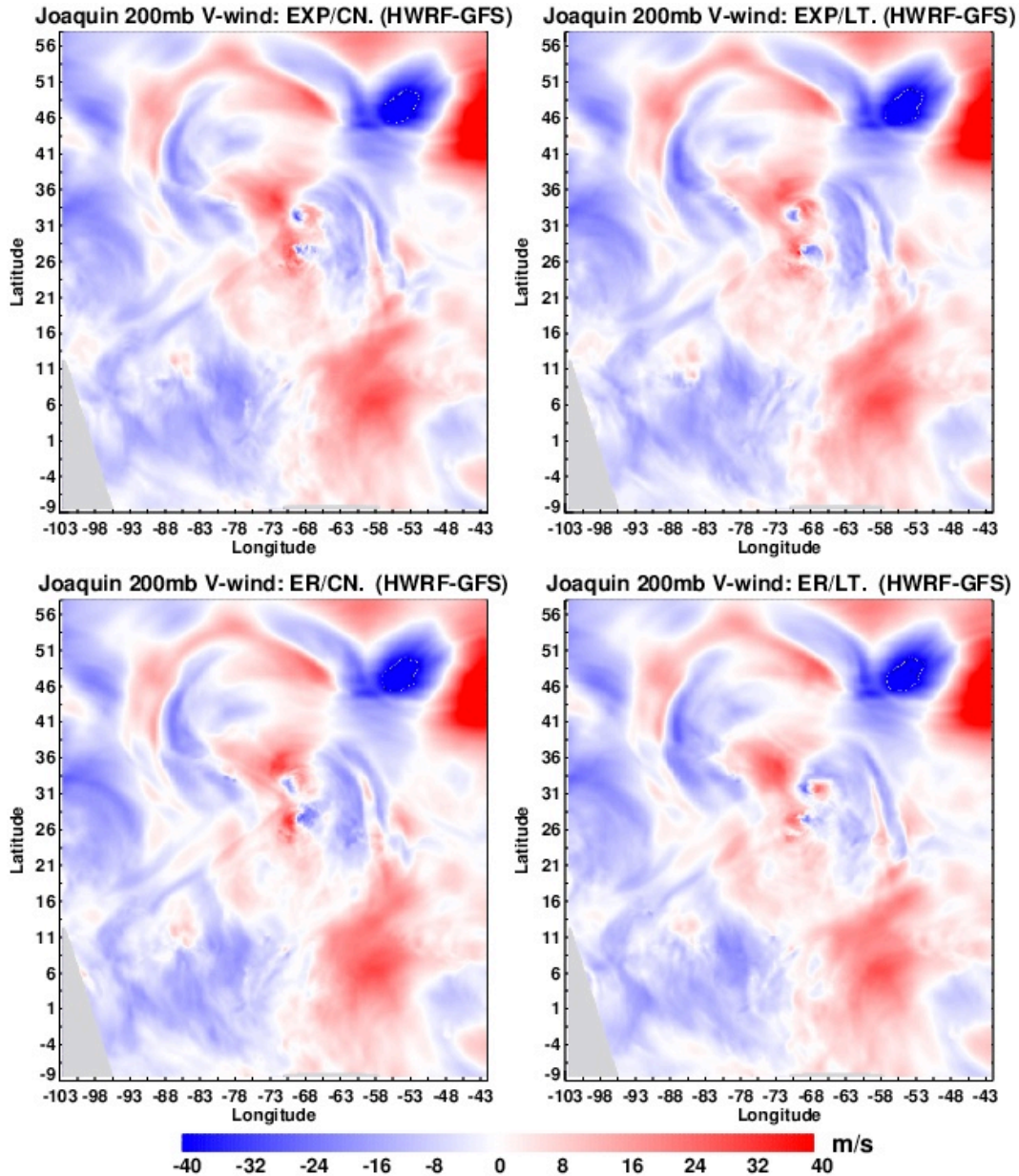
Figure 14. Meridional wind differences at 200 hPa of the synoptic environment around Hurricane Joaquin at 00 UTC on 4 October 2015 between H218 96-hour predictions at that forecast time and the GFS analysis at that time with H218 using EXP overlap with constant decorrelation length (top left), using EXP overlap with a latitude-varying decorrelation length (top right), using ER overlap with constant decorrelation length (bottom left), and using ER overlap with a latitude-varying decorrelation length (bottom right). Units are ms^{-1}. Gray areas denote missing data.

to the east of Irma (centered near 18°N and 45°W) is not only warmer in H218 than analyzed by GFS, but there are also noticeable differences among the EXP and ER overlap configurations in the H218 predictions suggesting some process in this area that was especially sensitive to the cloud overlap treatment.
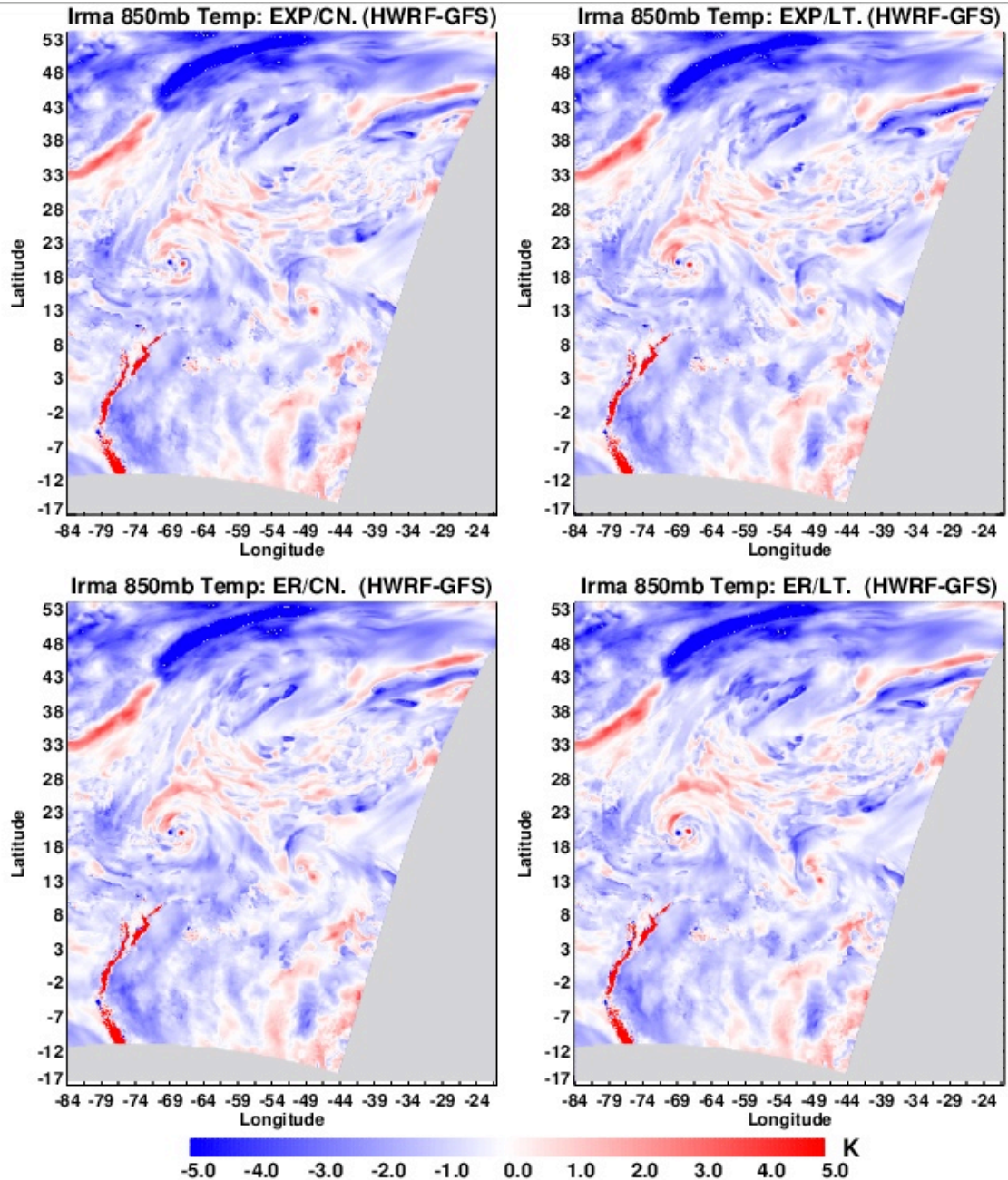
Figure 15. Temperature differences at 850 hPa of the synoptic environment around Hurricane Irma at 12 UTC on 7 September 2017 between H218 96-hour predictions at that forecast time and the GFS analysis at that time with H218 using EXP overlap with constant decorrelation length (top left), using EXP overlap with a latitude-varying decorrelation length (top right), using ER overlap with constant decorrelation length (bottom left), and using ER overlap with a latitude-varying decorrelation length (bottom right). Units are K. Gray areas denote missing data.
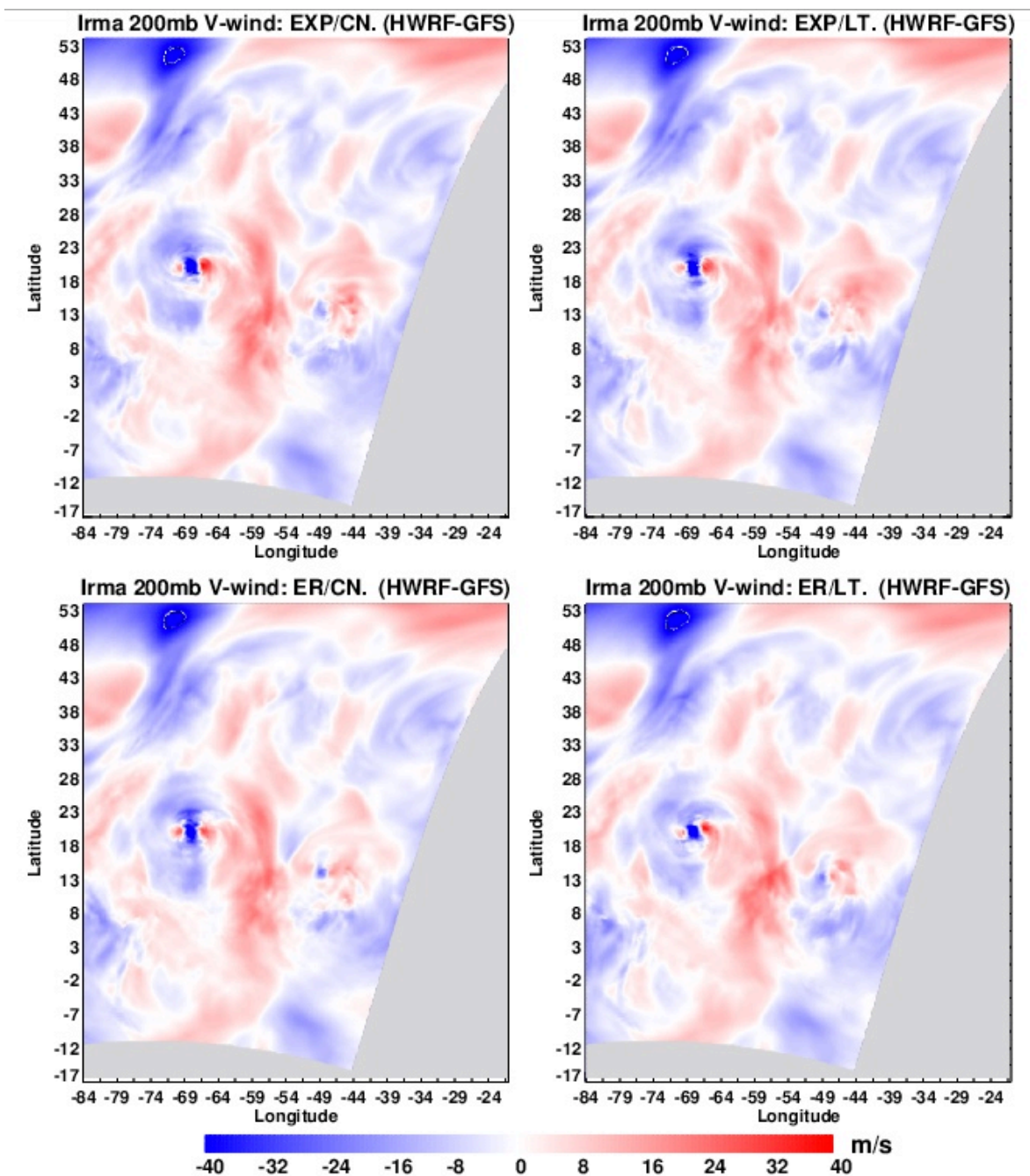
Figure 16. Meridional wind differences at 200 hPa of the synoptic environment around Hurricane Irma at 12 UTC on 7 September 2017 between H218 96-hour predictions at that forecast time and the GFS analysis at that time with H218 using EXP overlap with constant decorrelation length (top left), using EXP overlap with a latitude-varying decorrelation length (top right), using ER overlap with constant decorrelation length (bottom left), and using ER overlap with a latitude-varying decorrelation length (bottom right). Units are ms^{-1}. Gray areas denote missing data.

Atmospheric Impacts: Simulated Brightness Temperature

Tropical cyclone predictions can also be evaluated using simulated satellite brightness temperatures (*Otkin, et al.,* 2017). To illustrate the impact of changing the cloud overlap method on TC development, we examined the modeled 6.5 µm brightness temperatures generated during our H218 runs by the Unified Post Processor (UPP) for the storm-following output grid (labelled "*storm*" in the generated output files). Figure 17 shows the brightness temperature (BT) in the vicinity of Hurricane Irma at 12 UTC on 7 September 2017, which was forecast hour 96 from a forecast cycle initialized at 12 UTC on 3 September 2017. Although BT data for part of the scene are missing for this time, most of Hurricane Irma and its environment to the north, east and south are visible. The four panels in Figure 17 show the H218 simulated BT for four cloud overlap configurations including EXP overlap using a constant decorrelation length of 2500 m (top left), EXP using a latitude-varying decorrelation length (top right), ER using a constant decorrelation length of 2500 m (bottom left) and ER using a latitude varying decorrelation length (bottom right). BT data over the left portion of each panel (roughly west of 70°W) were missing from the simulated product. At this time, Irma had a best track minimum pressure of 921 mb with maximum sustained winds of 165 mph, and the hurricane was about 24-30 hours past its peak intensity. Even during this very mature stage, the appearance of Irma shows notable differences among the four cloud overlap methods including the extent of the coldest BTs within the central overcast, the extent of cold, high clouds in the outflow around the periphery of the storm, and the magnitude of higher BT in the surrounding environment to the northeast to southeast of Irma and even within the eye itself. The scope of this project prevented a comparison of the simulated BT to the observed values, though this insightful diagnostic will be utilized in future research.

To illustrate the evolution of BT within this scene over the course of a full forecast cycle, we examined brightness temperatures averaged over the entire scene (including only available data points). Figure 18 shows the time series of scene-averaged 6.5 µm BT for two H218 forecast cycles of Hurricane Irma initialized at 12 UTC on 3 September 2017 (top) and at 00 UTC on 6 September 2017 (bottom) using the same four cloud overlap configurations presented in Figure 17. In the earlier forecast cycle, the area-average BTs remain similar during the intensification occurring in the model at this time, then begin to diverge as Irma reaches its peak intensity in these simulations. The forecast using the ER/latitude-varying cloud overlap method halted its intensification somewhat earlier than the others, as indicated by its warmer BT, which (at 96 hours) is consistent with the BTs presented in Figure 17. In the later forecast cycle in Figure 18, the scene-averaged BTs also begin to diverge after the strongest period of intensification during day three with further differences appearing toward the end of the forecast cycle.
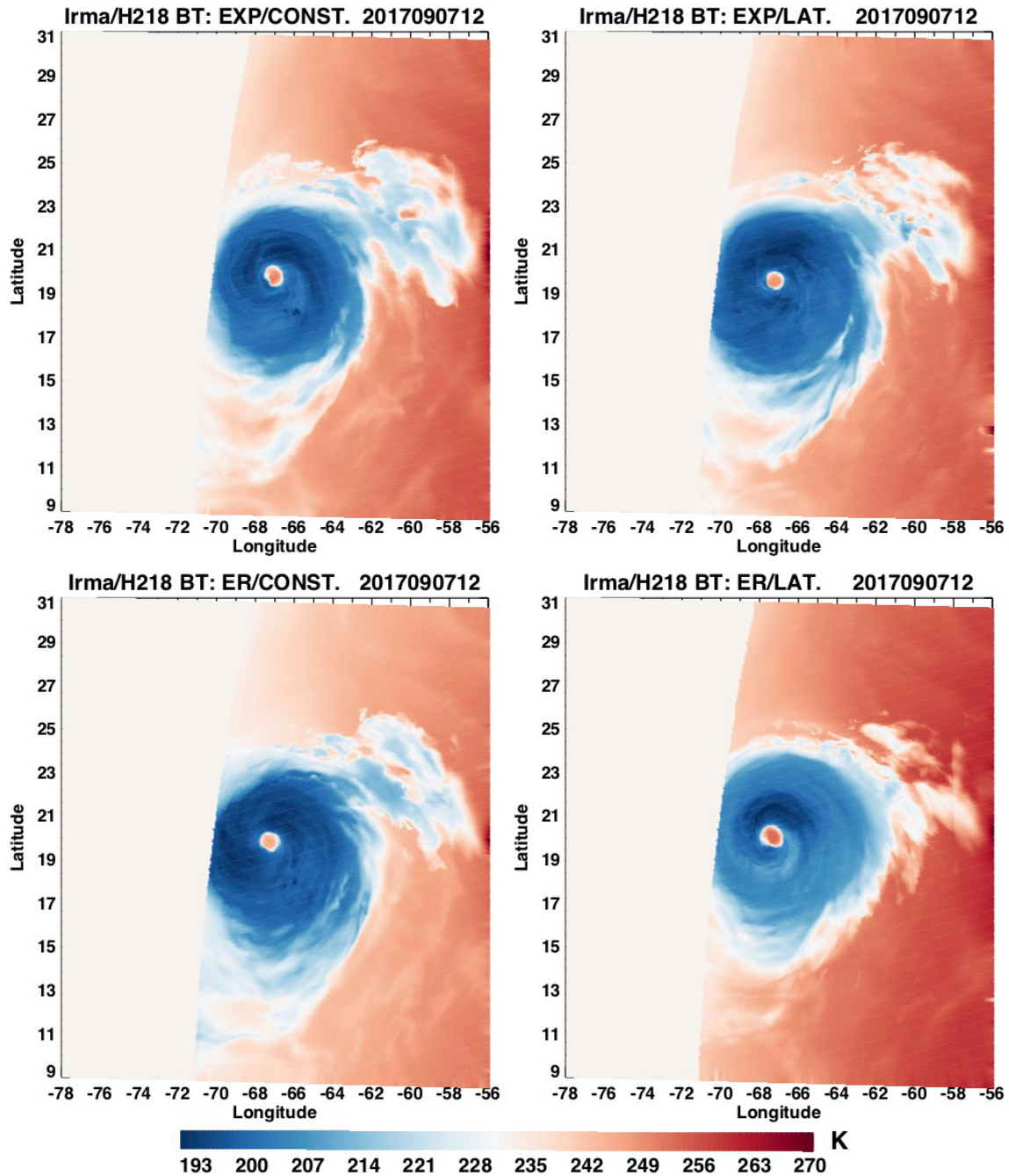
Figure 17. H218 simulated 6.5 µm brightness temperature in the vicinity of Hurricane Irma at 12 UTC on 7 September 2017 (96 hours into a forecast cycle initialized at 12 UTC 3 September 2017 as predicted using four versions of the DTC/H218 model using EXP cloud overlap with constant decorrelation length (top left), using EXP overlap with a latitude-varying decorrelation length (top right), using ER overlap with constant decorrelation length (bottom left), and using ER overlap with a latitude-varying decorrelation length (bottom right). Data over the left portion of each panel are missing. Units are in K.
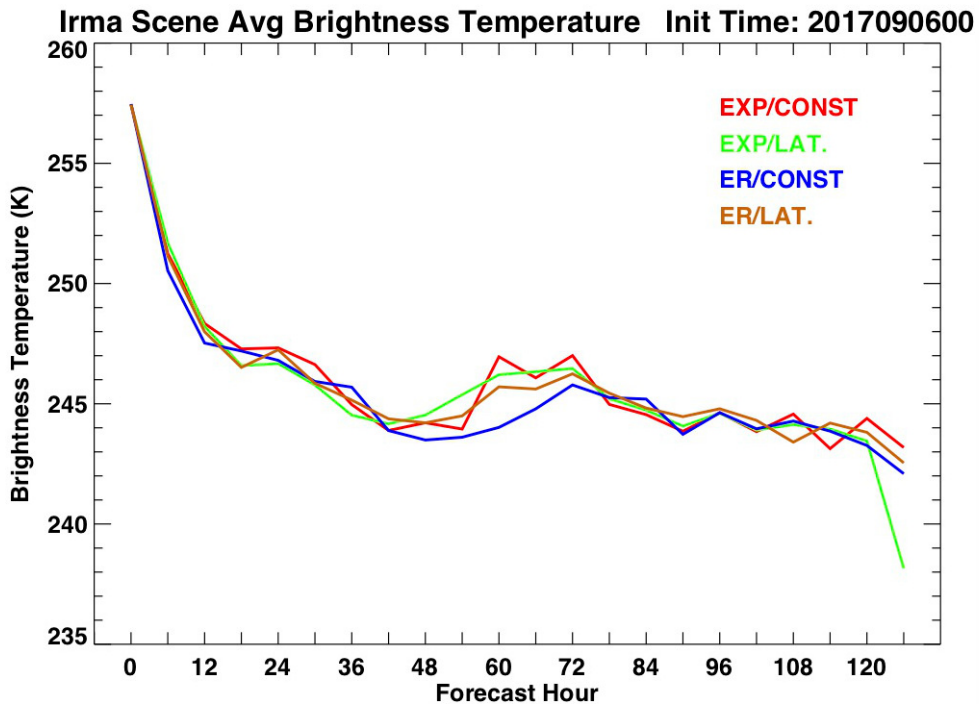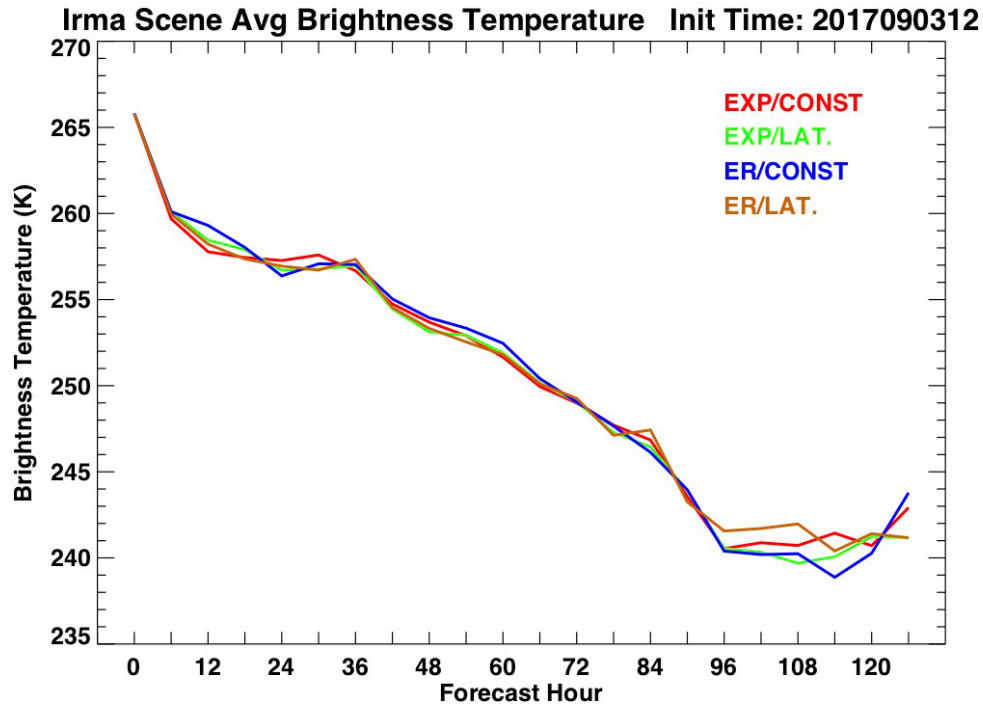
Figure 18. H218 simulated scene-averaged 6.5 μm brightness temperature in the vicinity of Hurricane Irma at each forecast time for a forecast cycle initialized at 12 UTC 3 September 2017 (top) and a forecast cycle initialized at 00 UTC 6 September 2017 (bottom) as predicted using four versions of the DTC/H218 model using EXP cloud overlap with constant decorrelation length (red), using EXP overlap with a latitude-varying decorrelation length (green), using ER overlap with constant decorrelation length (blue), and using ER overlap with a latitude-varying decorrelation length (gold).

Tropical Cyclone Track and Intensity Impacts

An important objective of improving tropical cyclone predictions is to increase TC track and intensity forecast skill. The previous sections have shown that enhancements to the radiative cloud overlap method can have significant impacts on radiative heating rates and atmospheric fields, and this section will illustrate the degree to which these overlap changes also influence the track and intensity of several of the TCs examined in this study. Establishing whether any of the new cloud overlap methods will improve the operational HWRF forecast skill will require testing by DTC and NOAA on a scale that is beyond the scope of this study. Our goals are to demonstrate that the impact on TC prediction is of sufficient magnitude in a least some meteorological contexts to justify this larger scale testing and to provide some guidance on which of the new cloud overlap methods to prioritize during potential future testing. The track and intensity plots to follow were derived from forecasts completed during this project of several recent tropical cyclones using the DTC/H218 version of HWRF.

As plotted by the GFDL vortex tracking software, Figure 19 shows the track of Hurricane Joaquin for a pair of five-day forecast cycles initialized at 00 UTC on 30 September 2015 (left panel) and at 00 UTC on 1 October 2015 (right panel) as originally predicted by HWRF using the 2015 operational version of the model ("HWRF", green) and predicted with H218 using ER overlap with latitude-varying decorrelation length ("C851", blue), using ER overlap with a constant decorrelation length of 2500 m ("C850", red), using EXP overlap with latitude-varying decorrelation length ("C841", yellow), and using EXP overlap with a constant decorrelation length of 2500 m ("C840", purple). The best track analysis position of the center of Hurricane Joaquin is shown in black in both panels of Figure 19. It should be noted that the 2015 operational HWRF used RRTMG with MR cloud overlap. For both forecast cycles, the H218 runs with EXP and ER bring the TC track much further eastward relative to the original HWRF prediction using MR overlap. Clearly, additional physics changes between 2015 and 2018 other than those added for this project may have contributed to the improvement seen in the more recent runs. However, the wide spread in the predictions after a couple of days with the four variations of the H218 model, which vary only in the cloud overlap method used, clearly illustrate the high sensitivity of this TC case to the cloud overlap process. During this time, Joaquin was interacting with a strong trough developing to its west over eastern North America.
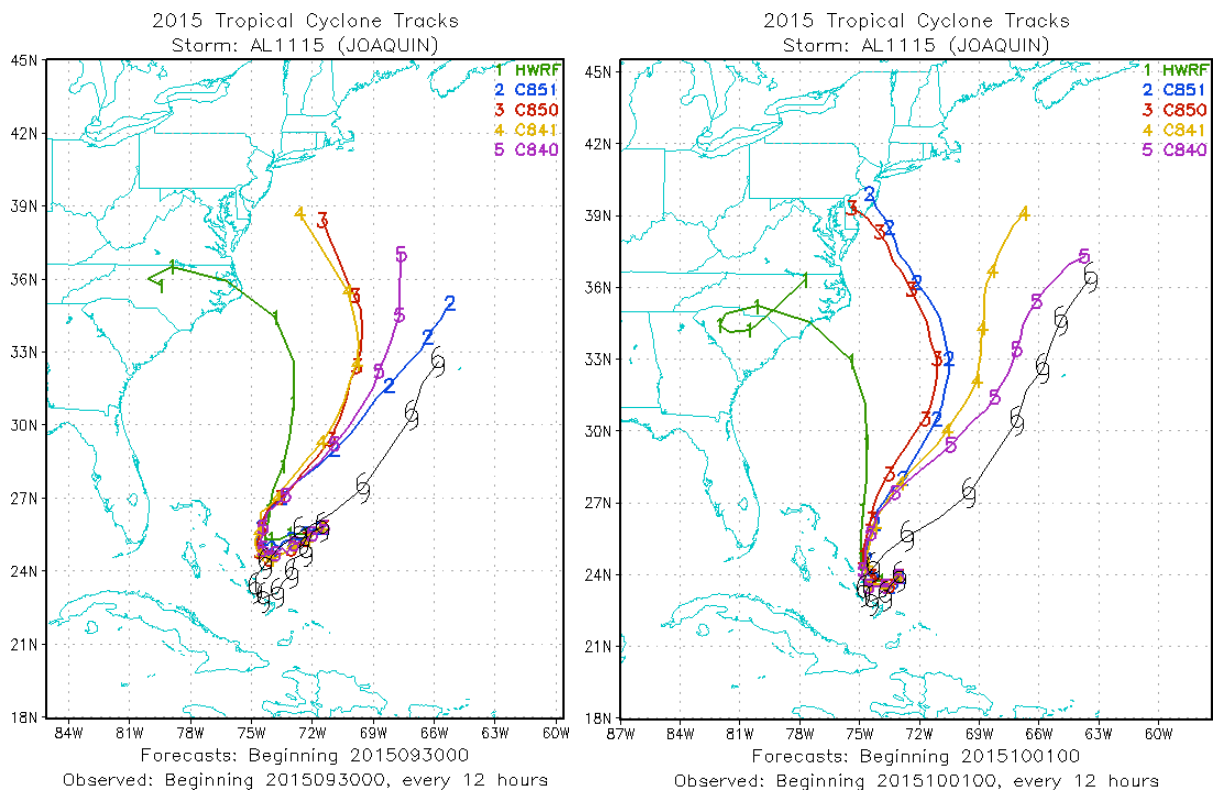
Figure 19. Hurricane Joaquin track over five-day forecast cycles starting at 00 UTC 30 September 2015 (left) and at 00 UTC on 1 October 2015 (right) as predicted using five versions of HWRF including the 2015 NOAA/EMC operational version ("HWRF", green), and the DTC/H218 version using ER overlap with latitude-varying decorrelation length ("C851", blue), using ER overlap with a constant decorrelation length ("C850", red), using EXP overlap with latitude-varying decorrelation length ("C841", yellow), and using EXP overlap with a constant decorrelation length ("C840", purple). Also shown is the best track analyzed position of Hurricane Joaquin over the same time period (black).

Tropical cyclone intensity is typically diagnosed through the TC minimum surface pressure and maximum surface wind speed. Time series of the minimum central surface pressure for Hurricane Joaquin as predicted by the same five versions of HWRF presented in Figure 19 are shown in the top panel of Figure 20 for the forecast cycle initialized at 00 UTC on 30 September 2015. The comparable time series of maximum sustained surface wind speeds for the same forecast cycle and model predictions are shown in the bottom panel of Figure 20. The analyzed surface pressures and wind speeds are also shown in Figure 20. During this forecast period, Joaquin quickly intensified during the first two days, then weakened thereafter due in part to its interaction with the Bahamas. The "HWRF" prediction using the 2015 operational model shows a drastically weaker storm during the last day due to its landfall over the eastern United States. Since they all remain over the ocean during this cycle, the two EXP and two ER predictions become stronger than the observed hurricane during days three and four before weakening. Other than these intensity differences due to the large track discrepancies, the wide range of intensities predicted during this cycle by the EXP and ER overlap methods suggests the strong sensitivity of the cloud

29
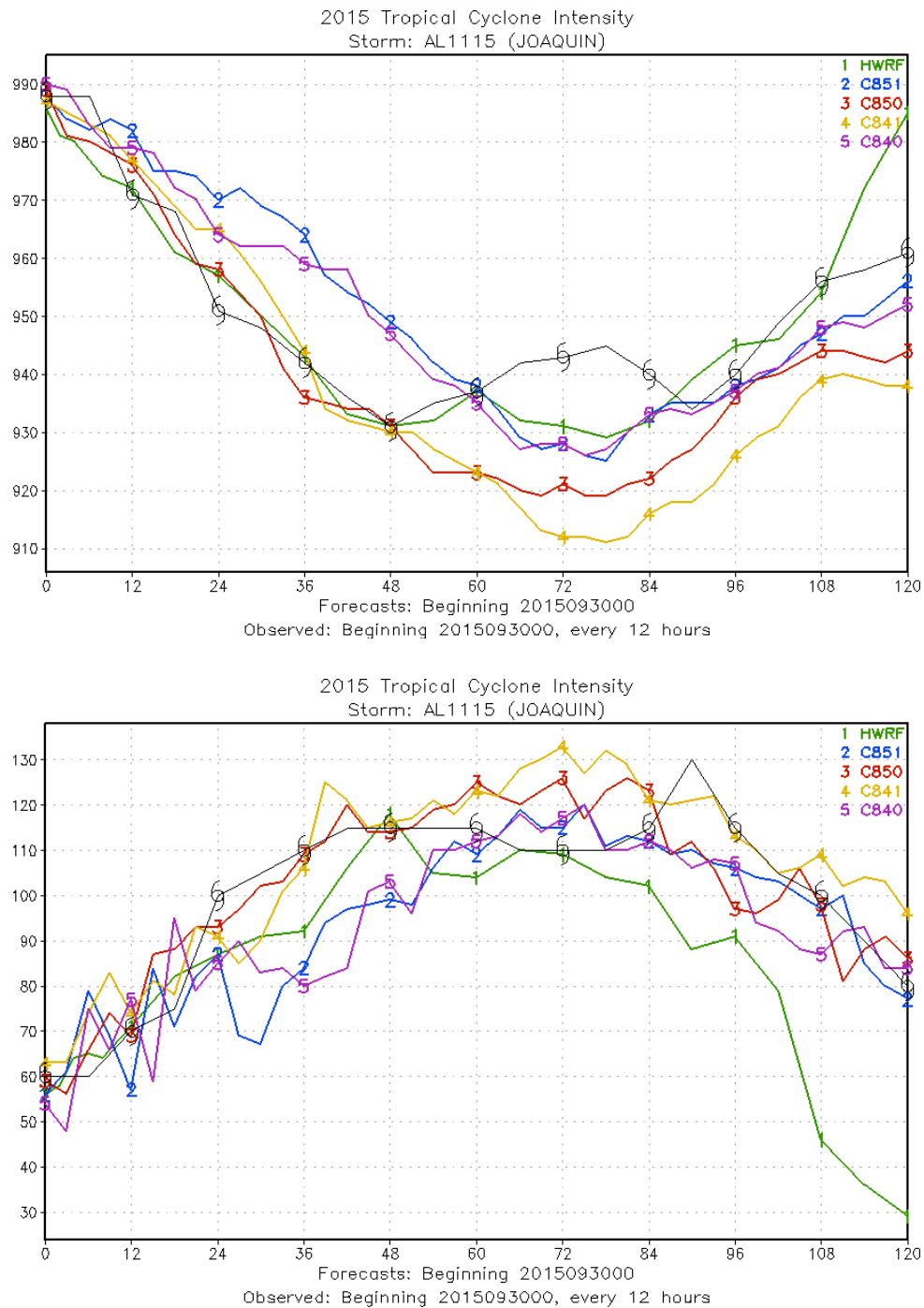
Figure 20. Hurricane Joaquin minimum surface pressure (top) and maximum wind speed (bottom) for a forecast cycle initialized at 00 UTC on 30 September 2015 as predicted using five versions of HWRF including the 2015 NOAA/EMC operational version ("HWRF", green), and the DTC/H218 version using ER overlap with latitude-varying decorrelation length ("C851", blue), using ER overlap with a constant decorrelation length ("C850", red), using EXP overlap with latitude-varying decorrelation length ("C841", yellow), and using EXP overlap with a constant decorrelation length ("C840", purple). Also shown is the best track analyzed position of Hurricane Joaquin over the same time period (black). The x-axis unit is hours and the y-axis units are hPa in the top panel and knots in the lower panel.

30

overlap impact to the specific features of the synoptic environment that controlled the evolution of Joaquin during this time.

The impact of the cloud overlap change on the predicted track of Hurricane Irma over two forecast cycles initialized at 12 UTC on 5 September 2017 and at 00 UTC on 6 September 2017 is shown in Figure 21. In these panels, "HWRF" refers to the tracks as predicted by the 2017 operational version of HWRF, which used RRTMG with MR cloud overlap. In each case, the predicted tracks remained generally north of the observed track, with the exception of the "HWRF" forecast during the earlier cycle in which Irma drifted south of the observed track and further inland over northern Cuba. It is notable that track differences among the EXP and ER predictions are negligible until the latter days of each cycle when the models were attempting to predict the northward turn of the TC between Cuba and Florida as it began to interact with a trough over the Gulf of Mexico. This once again suggests the sensitivity of the overlap impact to the presence of mid-latitude synoptic features in the vicinity of the tropical cyclone.

Time series of the minimum central surface pressure for Hurricane Irma as predicted by the same five versions of HWRF and the same two forecast cycles presented in Figure 21 are shown in Figure 22. The predictions diverge from the observed intensity most significantly during days four and five in each cycle, largely due to the proximity of the TC to land in each case. The four forecasts using the EXP and ER overlap methods are only minimally impacted by land over these cycles, and they remain close to or somewhat more intense than the observed intensity with the exception of the ER overlap forecast using the latitude-varying decorrelation length ("C851"), which is somewhat weaker than the observed intensity (and the other EXP and ER cases) during days two to four. The reason for the deviation of the "C851" case has not been established, though it hints at the impact on TC evolution of the subtle cloud overlap changes examined in these tests.

As a final example of track and intensity impacts, the effect of the cloud overlap change on the predicted track of Hurricane Florence over two forecast cycles initialized at 12 UTC on 3 September 2018 and at 12 UTC on 8 September 2018 is shown in Figure 23. In these panels, "HWRF" refers to the tracks as predicted by the 2018 operational version of HWRF, which was updated by NOAA to use RRTMG with the EXP cloud overlap and a constant decorrelation length of 2500 m (our "C840" overlap configuration). For this reason, we limited our testing of Hurricane Florence to ER overlap with the constant and latitude-varying decorrelation length. It should be noted that there may be additional physics differences between the 2018 operational HWRF and the DTC/H218 model used for our testing (in addition to the use of the GFS ensemble method for estimating the background error covariance for efficiency in our H218 forecasts). Figure 23 shows that the forecasts with ER overlap are each noticeably different from each other and from the EXP
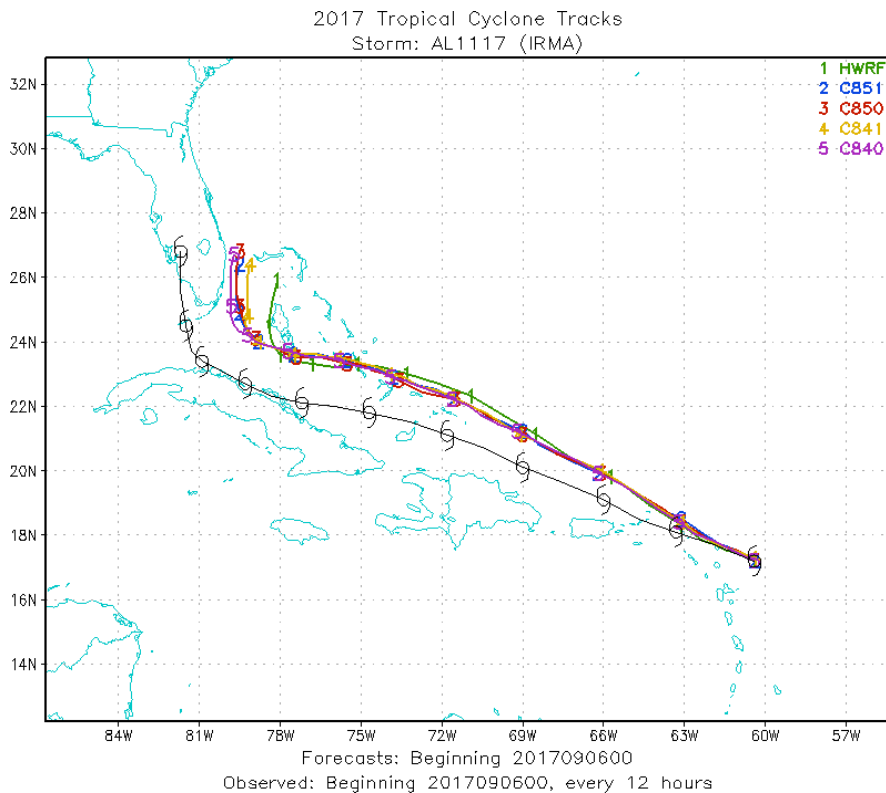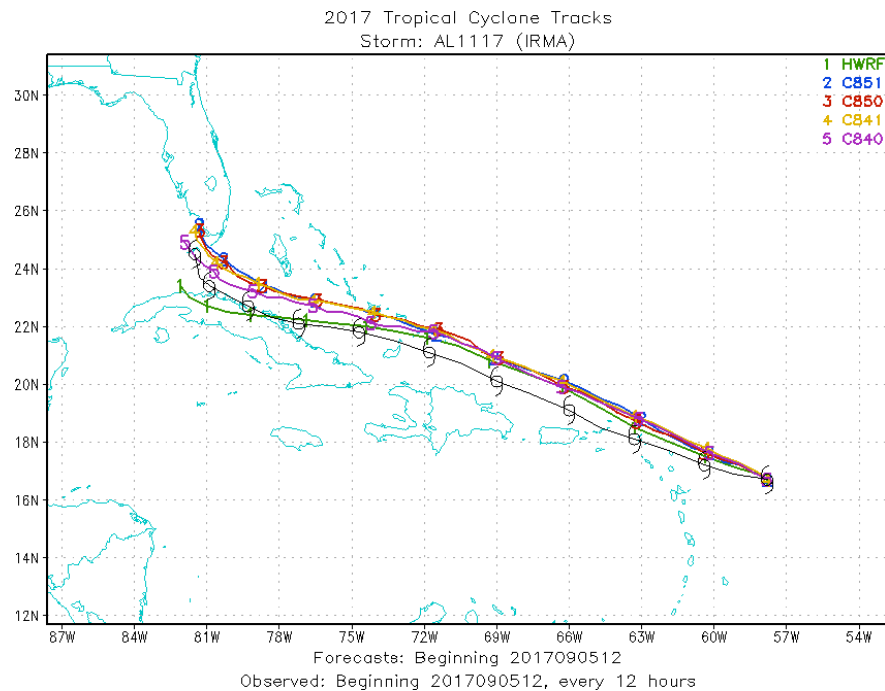
Figure 21. Hurricane Irma track over five-day forecast cycles starting at 12 UTC 5 September 2017 (top) and at 00 UTC on 6 September 2017 (bottom) as predicted using five versions of HWRF including the 2017 NOAA/EMC operational version ("HWRF", green), and the DTC/H218 version using ER overlap with latitude-varying decorrelation length ("C851", blue), using ER overlap with a constant decorrelation length ("C850", red), using EXP overlap with latitude-varying decorrelation length ("C841", yellow), and using EXP overlap with a constant decorrelation length ("C840", purple). Also shown is the best track analyzed position of Hurricane Irma over the same time period (black).
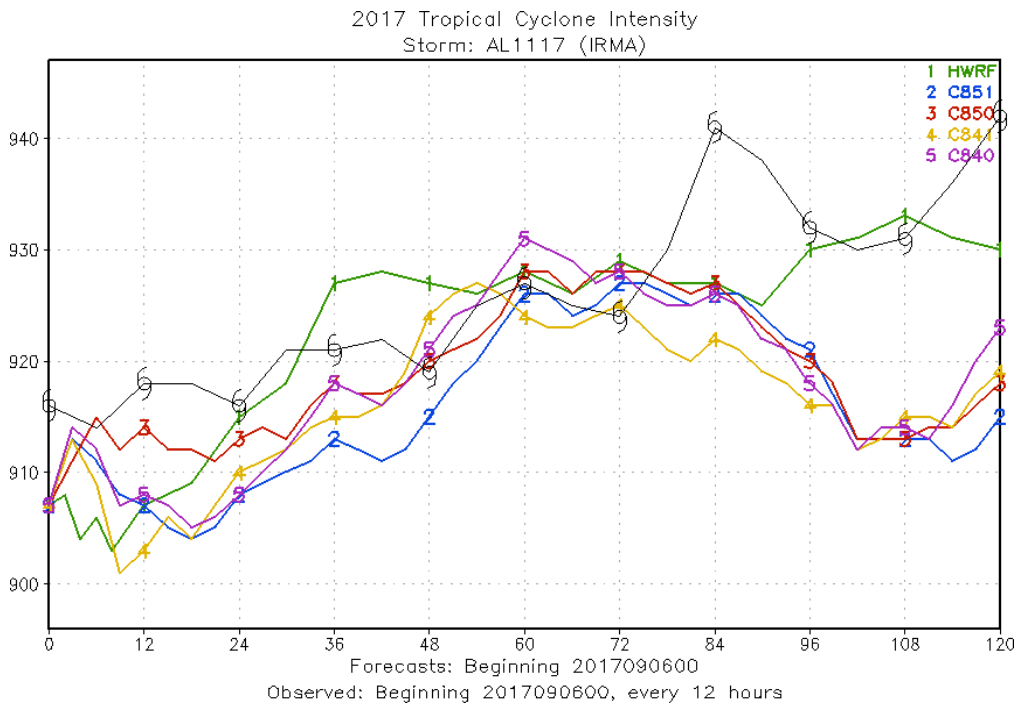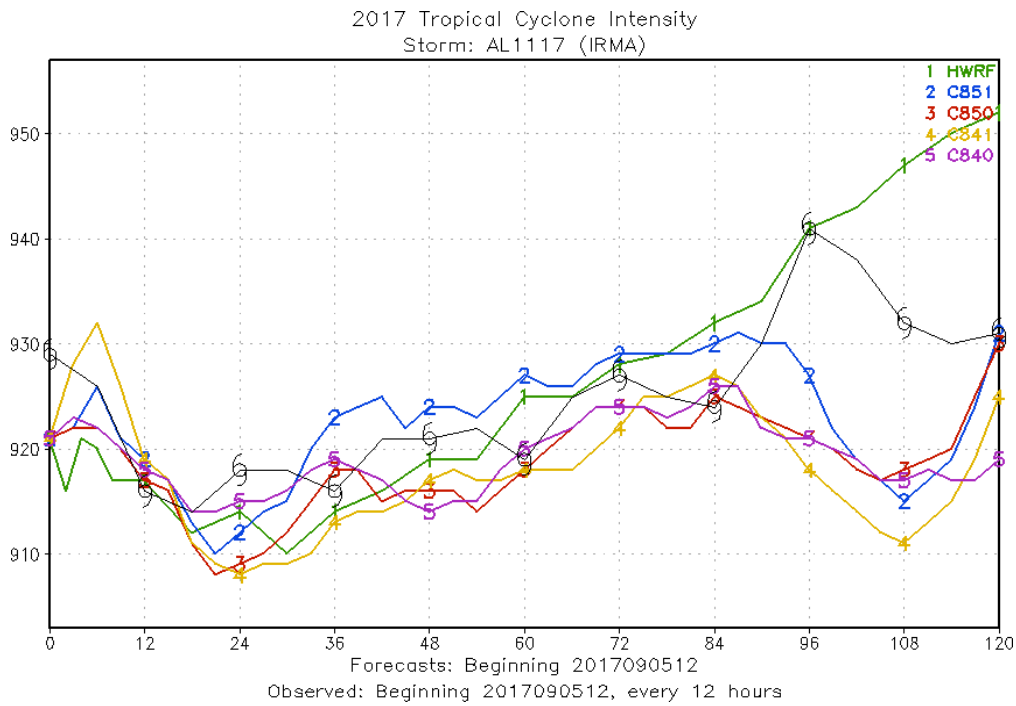
Figure 22. Hurricane Irma minimum surface pressure (top) and maximum wind speed (bottom) for a forecast cycle initialized at 00 UTC on 6 September 2017 as predicted using five versions of HWRF including the 2017 NOAA/EMC operational version ("HWRF", green), and the DTC/H218 version using ER overlap with latitude-varying decorrelation length ("C851", blue), using ER overlap with a constant decorrelation length ("C850", red), using EXP overlap with latitude-varying decorrelation length ("C841", yellow), and using EXP overlap with a constant decorrelation length ("C840", purple). Also shown is the best track analyzed surface pressure of Hurricane Irma over the same time period (black). The x-axis unit is hours and the y-axis units are hPa in each panel.

33
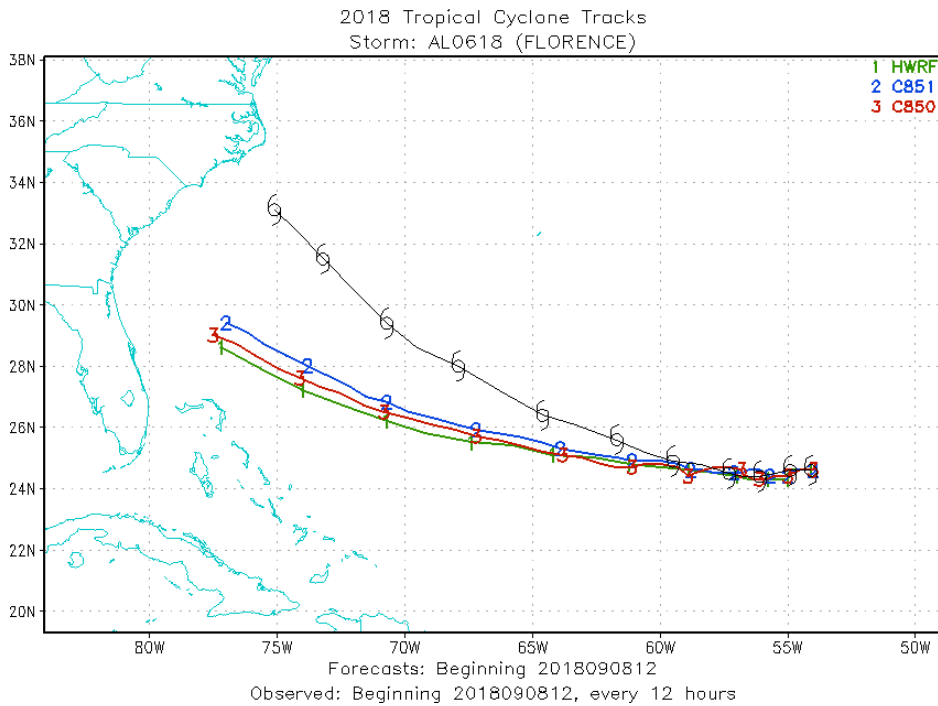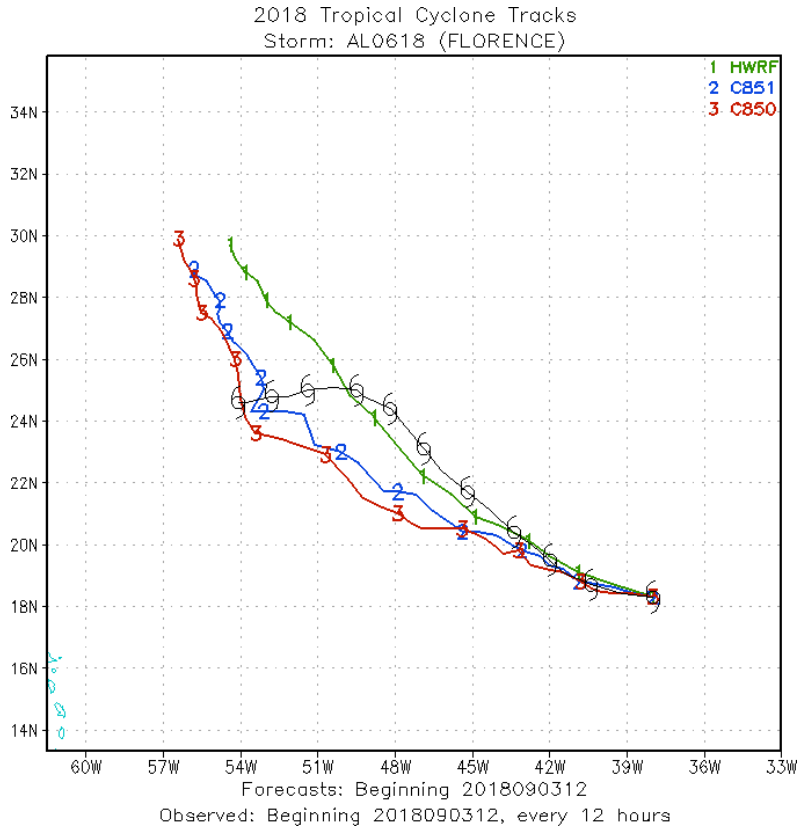
Figure 23. Hurricane Florence track over five-day forecast cycles starting at 12 UTC 3 September 2018 (top) and at 12 UTC on 8 September 2018 (bottom) as predicted using three versions of HWRF including the 2018 NOAA/EMC operational version ("HWRF", green), and the DTC/H218 version using ER overlap with latitude-varying decorrelation length ("C851", blue) and using ER overlap with a constant decorrelation length ("C850", red). Also shown is the best track analyzed position of Hurricane Florence over the same time period (black).

result, with the former being somewhat worse than EXP in one cycle and somewhat better in the other relative to the observed track. Forecasts of minimum surface pressure for the same two cycles and models are shown in Figure 24. It is very apparent in the upper panel of Figure 24 that the model predictions completely missed the short period of rapid intensification experienced by Florence during days 2 and 3 of this cycle. The models also missed the change in track seen in the top panel of Figure 23 during the last few days of the same forecast cycle. Whatever the cause of these lapses, the overlap methods produced different results, which again suggests their influence on and sensitivity to environmental factors that affect TC evolution.
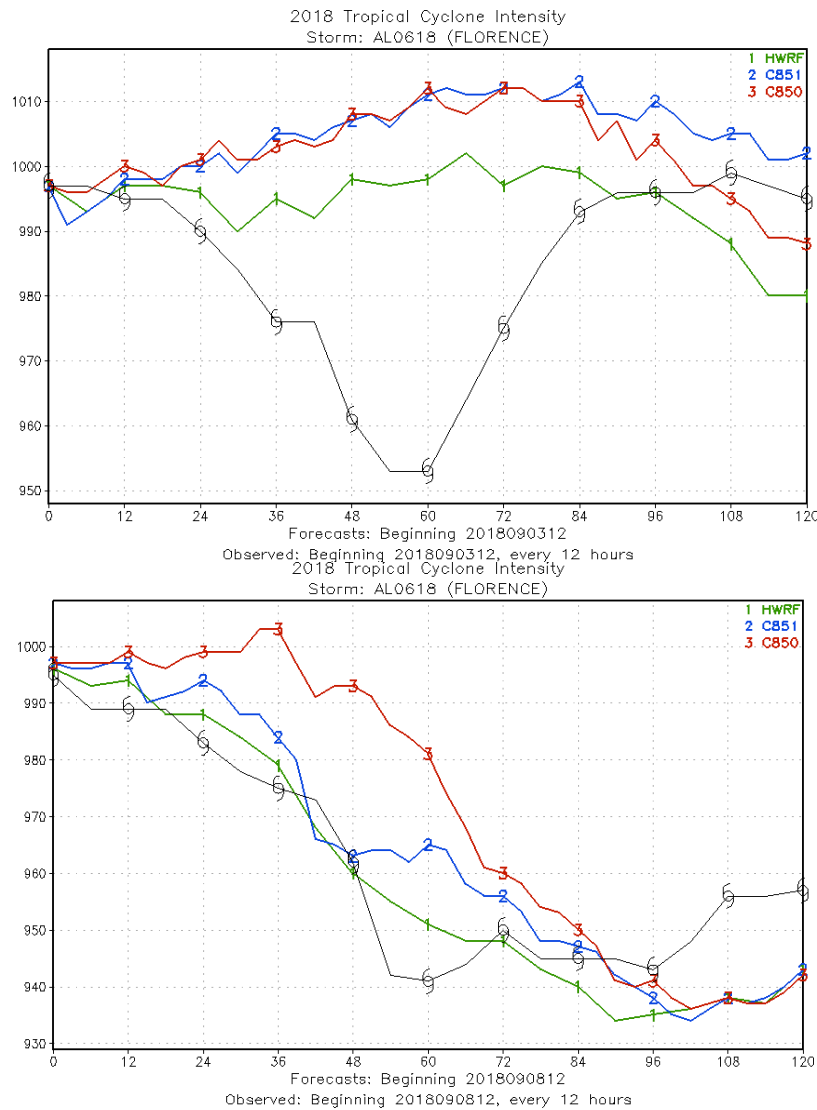
Figure 24. Hurricane Florence minimum surface pressure for two forecast cycles initialized at 12 UTC on 3 September 2018 (top) and 12 UTC on 8 September 2018 (bottom) as predicted using three versions of HWRF including the 2018 NOAA/EMC operational version ("HWRF", green), and the DTC/H218 version using ER overlap with latitude-varying decorrelation length ("C851", blue) and using ER overlap with a constant decorrelation length ("C850", red). Also shown is the best track analyzed surface pressure of Hurricane Florence over the same time period (black). The x-axis unit is hours and the y-axis units are hPa in each panel.

35

4. Conclusions and Future Work

The goal of this project was to illustrate the potential for modifications to the cloud overlap treatment applied in the radiation code to influence the radiative fluxes and heating rates, the atmospheric state, and ultimately the track and intensity of tropical cyclones predicted by HWRF. The additional cloud overlap method tested is an extension of the exponential method studied in our previous research known as exponential-random cloud overlap. The ER method relaxes the strict assumption of maximum overlap through adjacent cloud layers by allowing the vertical correlation of clouds to transition exponentially from maximum to random with distance through the cloud (which EXP also does) while also enforcing random overlap between non-adjacent blocks of cloudy layers (which EXP does not do). Both a constant decorrelation length scale of 2.5 km and a latitude-varying decorrelation length were tested in the TC forecasts completed for this project. However, the selection of the optimal decorrelation length to use at a given latitude or for a specific cloud configuration or atmospheric state requires further research. The physics changes were tested using both the H217 and H218 DTC versions of HWRF (with the ICLOUD=3 name-list option for defining fractional cloudiness) and the RRTMG longwave and shortwave radiation codes. Forecasts using the EXP and ER cloud overlap methods and both decorrelation length specifications were completed for multiple forecast cycles of recent Hurricanes Joaquin, Harvey, Irma and Florence.

Several primary conclusions can be drawn from the work completed during this project. First, it was shown that simulated radiative heating rate profiles reflect the influence of all of the atmospheric state variables ingested into the radiation code and provide detailed information related to the inner structure of tropical cyclones, though heating rate verification options remain limited. Second, the relative effects of EXP and ER overlap are similar in comparison to each other in contrast to the larger difference between each of these methods and the original MR overlap approach. Third, the newly tested ER overlap, due to its similar enforcement of random overlap between non-adjacent cloudy layers while relaxing the strict application of maximum overlap in adjacent cloudy layers, is the logical successor to the widely used MR overlap and should be prioritized in further testing. Fourth, through their effect on heating rates, both EXP and ER influence the atmospheric state in the vicinity of developing TCs and within the surrounding synoptic environment over time as seen in their effect on temperatures, wind speeds, brightness temperatures, and other parameters. Finally, subsequent impacts on hurricane track and intensity are highly variable, though a pattern is emerging from our analysis that TC track and intensity influences due to changes in the cloud overlap process may be more likely when hurricanes are in the vicinity of mid-latitude synoptic features (especially those that support cloudiness) as opposed to when they are moving unimpeded over the open ocean.

36

Given the magnitude of the changes to the atmospheric environment and TC track and intensity seen in the cases studied for this project, the implications of effectively treating the radiative influence of the vertical correlation of fractional clouds (as well as the parameterization of fractional cloudiness itself) continue to require further investigation. Work is pending within the DTC and at EMC to evaluate the ER cloud overlap for a larger number of TC cases to provide a better statistical basis for assessing its impact. Our project also resulted in the addition of name-list options to HWRF that can be used to select the cloud overlap type (MR, EXP or ER) and to select the decorrelation length type for the exponential methods (constant or latitude-varying) in support of DTC and EMC testing of these options. Finally, future research will investigate the benefit of developing more sophisticated rules for spatially selecting both the cloud overlap type and the decorrelation length in ways that effectively reflect the dependence of cloud vertical correlation and its important radiative influence on the atmospheric state.

5. Project Deliverables

This project generated several code related deliverables and accomplishments for the DTC and NOAA including:

1) Source code for exponential-random cloud overlap was added to HWRF/RRTMG,
2) Source code for the latitude-varying decorrelation length capability for the EXP and ER overlap methods was added to HWRF/RRTMG,
3) Input control name-list options for the cloud overlap type and the decorrelation length type were added to HWRF to facilitate testing of these options at DTC and EMC,
4) The previously delivered exponential cloud overlap source code was adopted by NOAA during this project for operational use in HWRF for the 2018 hurricane season.

In addition, one presentation (an AMS Conference poster), the final project report (this document), and contributions to the HWRF 2018 (v4.0a) scientific documentation were delivered:

1) Henderson, J., M. Iacono, M. Biswas, E. Kalina, K. Newman, B. Liu, and Z. Zhang, Impact of revisions to RRTMG cloudy radiative transfer on tropical cyclone evolution in HWRF, Poster presentation at the 33rd American Meteorological Society Conference on Hurricanes and Tropical Meteorology, Ponte Vedra, Florida, April 16-20, 2018.
2) Iacono, M.J., and J.M. Henderson, Testing variations of exponential-random cloud overlap with RRTMG in HWRF, Project Final Report, Developmental Testbed Center, February 2019.
3) Biswas, M.K., S. Abarca, L. Bernardet, I. Ginis, E. Grell, M. Iacono, E. Kalina, B. Liu, Q. Liu, T. Marchok, A. Mehra, K. Newman, J. Sippel, V. Tallapragada, B. Thomas, W. Wang, H. Winterbottom, and Z. Zhang, Hurricane Weather Research and Forecasting (HWRF) Model: 2018 Scientific Documentation, National Center for Atmospheric Research, Developmental Testbed Center, 103 pp, 2018.

6. References

Barker, H., J.N.S. Cole, J.-J. Morcrette, R. Pincus, P. Raisanen, Monte Carlo Independent Column Approximation (McICA): Up and running in North America and Europe, Talk presented at the 17th Atmospheric Radiation Measurement (ARM) Science Team Meeting, Monterey, CA, March 26-30, 2007.

Berg, R., National Hurricane Center Tropical Cyclone Report: Hurricane Joaquin (AL112015), National Hurricane Center, 36 pp., 2016.

Bernardet, L., V. Tallapragada, S. Bao, S. Trahan, Y. Kwon, Q. Liu, M. Tong, M. Biswas, T. Brown, D. Stark, L. Carson, R. Yablonsky, E. Uhlhorn, S. Gopalakrishnan, X. Zhang, T. Marchok, B. Kuo, and R. Gall, Community Support and Transition of Research to Operations for the Hurricane Weather Research and Forecasting Model. *Bull. Amer. Meteor. Soc.*, 96, 953–960, 2015.

Biswas, M.K., and co-authors, Hurricane Weather Research and Forecasting (HWRF) Model: 2017 Scientific Documentation, National Center for Atmospheric Research Technical Note NCAR/TN-544+STR, 2017.

Biswas, M.K., and co-authors, Hurricane Weather Research and Forecasting (HWRF) Model: 2018 Scientific Documentation, National Center for Atmospheric Research, Developmental Testbed Center, 103 pp, 2018.

Blake, E.S., and D.A. Zelinsky, National Hurricane Center Tropical Cyclone Report: Hurricane Harvey (AL092017), National Hurricane Center, 77 pp., 2018.

Cangialosi, J.P, A.S. Latto, and R. Berg, National Hurricane Center Tropical Cyclone Report: Hurricane Irma (AL112017), National Hurricane Center, 111 pp., 2018.

Geleyn, J.F., Hollingsworth. A., An economical, analytical method for the computation of the interaction between scattering and line absorption of radiation, *Contrib. Atmos. Phys.,* 52, 1–16, 1979.

Hogan, R.J., and A. Bozzo, ECRAD: A new radiation scheme for the IFS, Technical Memorandum 787, European Centre for Medium-Range Weather Forecasts, 33 pp., 2016.

Hogan, R.J., Illingworth, A.J., Deriving cloud overlap statistics from radar. *Q. J. R. Meteorol. Soc.*, 126, 2903–2909, 2000.

Iacono, M.J., J.S. Delamere, E.J. Mlawer, M.W. Shephard, S.A. Clough, and W.D. Collins, Radiative forcing by long-lived greenhouse gases: calculations with the AER radiative transfer models, *J. Geophys. Res.*, 113, D13103, doi:10.1029/2008JD009944, 2008.

Nam, C., S. Bony, J.-L. Dufresne, and H. Chepfer, The 'too few, too bright' tropical low-cloud problem in CMIP5 models, *Geophys. Res. Lett.*, 39, L21801, doi:10.1029/2012GL053421, 2012.

Otkin, J.A., W.E. Lewis, A.J. Lenzen, B.D. McNoldy, and S.J. Majumdar, Assessing the accuracy of the cloud and water vapor fields in the hurricane WRF (HWRF) model using satellite infrared brightness temperatures, *Mon. Weather Rev.*, 145, 2027-2046, 2017.

Pincus, R., C. Hannay, S. A. Klein, K.-M. Xu, and R. Hemler, Overlap assumptions for assumed probability distribution function cloud schemes in large-scale models, *J. Geophys. Res.*, 110, D15S09, doi:10.1029/2004JD005100, 2005.

Pincus, R., H. W. Barker, J.-J. Morcrette, A fast, flexible, approximate technique for computing radiative transfer in inhomogeneous cloud fields, *J. Geophys. Res.,* 108, D13, 2003.

Shonk, J.K.P., R.J. Hogan, J.M. Edwards, and G.G. Mace, Effect of improving representation of horizontal and vertical cloud structure on the Earth's global radiation budget. Part I: Review and parametrization, *Q. J. R. Meteorol. Soc.*, 136, 1191–1204, 2010a.

Shonk, J.K.P., and R.J. Hogan, Effect of improving representation of horizontal and vertical cloud structure on the Earth's global radiation budget. Part II: The global effects, *Q. J. R. Meteorol. Soc.,* 136, 1205–1215, 2010b.

Tourville, N., G. Stephens, M. DeMaria, and D. Vane, Remote Sensing of Tropical Cyclones: Observations from CloudSat and A-Train Profilers. *Bull. Amer. Meteor. Soc.*, **96**, 609–622, 2015.

Wu, X., and X.-Z. Liang, Radiative effects of cloud horizontal inhomogeneity and vertical overlap identified from a month-long cloud resolving simulation, *J. Atmos. Sci.*, 62, 4105–4112, 2005.